Acute and early stress axis modulation in joint disease permanently reduces pain and emotional comorbidities

Sara Hestehave[1,2], Roxana Florea[1], Samuel Singleton[3], Alexander J.H. Fedorec[1], Sara Caxaria[4], Oakley Morgan[1], Katharina Tatjana Kopp[5], Laurence A. Brown[6], Tim Heymann[7], Shafaq Sikandar[4], Felix Hausch[7,8], Stuart N. Peirson[9], Sandrine M. Géranton[1].

[1]Dept. of Cell & Developmental Biology, University College London, United Kingdom.

[2]Current address; Dept. Of Experimental Medicine, University of Copenhagen, Denmark.

[3]School of Medicine, University of Dundee, United Kingdom

[4]William Harvey Research Institute, Barts and The London School of Medicine and Dentistry, Queen Mary University, United Kingdom.

[5]Department of Pharmacy, Pharmaceutical Technology and Biopharmaceutics, Ludwig-Maximilians-Universität München, Munich, Germany.

[6]Research IT, University of Oxford, United Kingdom

[7]Institute of Organic Chemistry and Biochemistry, Technical University Darmstadt, Darmstadt, Germany.

[8]Centre for Synthetic Biology, Technical University Darmstadt

[9]Nuffield Department of Clinical Neuroscience, University of Oxford, United Kingdom.

*Corresponding author: Sandrine M. Géranton; Medawar Building, Dept. of Cell & Developmental Biology, University College London, WC1E 6BT, United Kingdom; Tel: +442036793386; https://profiles.ucl.ac.uk/10207; ORCID: 0000-0002-1659-1285; email: sandrine.geranton@ucl.ac.uk

Conflict-of-interest statement:

The authors have declared that no conflict of interest exists.

Abstract (200 words)

Chronic secondary musculoskeletal pain affects 20-30% of the population and includes sensory disturbances and emotional comorbidities, such as anxiety and depression, which reduce quality of life. We monitored a pre-clinical model of persistent joint pain for 6 months and found that sensory and functional changes were immediate while anxio-depressive comorbidities appeared from 3 months onwards. Modulating the stress axis *via* genetic deletion or pharmacological blockade of the stress driver FKBP51 reduced both sensory and emotional symptoms, including injury-induced disruptions in sleep and activity patterns, and did not worsen joint damage. FKBP51 pharmacological blockade after the establishment of the hypersensitive state provided temporary relief while acute inhibition at disease onset, when sensory and affective responses were most severe, provided at least 6 months of pain relief and reduced or prevented late anxiety- and depressive-like behavior. RNA sequencing suggested that FKBP51 inhibition at disease onset downregulated the *Naaa* gene in the superficial dorsal horn, a key regulator of the transition to chronic pain, and reorganized spinal cilia. Our findings suggest that acute and early, but not late, FKBP51 targeting can offer permanent relief from chronic pain and its emotional effects, highlighting the importance for fast therapeutic intervention.

Introduction

Living with chronic pain, which is defined as pain that lasts for more than 3 months, often means reduced quality of life due to significant negative affective symptoms such as suffering, anxiety, depression and disrupted sleep, comorbidities which can exacerbate each other (1–3). These various aspects of the pain experience tend to be clinically addressed individually and their management is usually poor, with treatments showing little to no efficacy (4). Conventional drug therapies for chronic pain are also often accompanied by significant side-effects that stop patients from seeking medication. Overall, despite recent advances in our understanding of the mammalian brain circuits that contribute to the different aspects of chronic pain, we are still looking for effective therapies that would improve patients' quality of life. This is likely to be because pre-clinical studies of chronic pain have so far mainly focused on the early sensory impact of chronic pain, with only very few studies looking at both sensory and affective symptoms at time points more relevant to the human chronic condition. However, we have now fully characterised an animal model of persistent joint pain, the MIA model (5), that induces joint damage similar to osteoarthritis (OA), with animals displaying sensory and affective symptoms, as experienced by chronic pain patients, which allows us to explore novel approaches for long-term pain management.

The protein FKBP51 was recently highlighted as a crucial driver of chronic pain in rodents, where it acts at the level of spinal pain circuits known to generate widespread pain in chronic pain states (6–8). Moreover, genetic variations in *FKBP5* influence the severity of musculoskeletal pain symptoms experienced by humans after trauma, suggesting a universal role for FKBP51 in chronic pain (9–11). The protein FKBP51 modulates the glucocorticoid receptor sensitivity and is important for the regulation of the stress response. High levels of FKBP51 protein tend to be associated with a hyper-reactive stress pathway often seen in patients with depression, while low levels of FKBP51 dampen-down the stress pathway and produce a more robust and resilient individual (12). Supporting these observations, deletion of FKBP51 in healthy mice has independently been shown to reduce anxiety-related behaviour (13, 14) and improve sleep quality (15). Altogether, these observations suggest that blocking FKBP51 in chronic pain patients could help with the management of many symptoms associated with poor quality of life. Importantly, studies with *Fkbp5* KO mice have shown that key physiological parameters such as life span (16),

reproduction (13, 15, 17–19), locomotion (7, 14, 17, 18), feeding (17, 20) and acute pain perception (6, 7) are unaltered, suggesting very mild, if any, side effects of a putative FKBP51-directed pharmacotherapy. Following our previous success with FKBP51-manipulation to reduce hypersensitivity in persistent pain states (6, 7), our hypothesis was that pharmacologically targeting the stress axis through the protein FKBP51 could be a novel clinical approach for the management of sensory, functional and emotional symptoms associated with chronic joint pain. Moreover, we have recently demonstrated that the early stage of persistent pain can predict the intensity of later emotional comorbidities (5). Therefore, we also anticipated that early treatment through FKBP51 inhibition would improve long-term emotional comorbidities.

We have developed the first selective antagonists of FKBP51 described so far (21). Acute administration of these antagonists recapitulates the anxiolytic properties of FKBP51 deletion in mice (13). We have previously pre-clinically tested one of these compounds, SAFit2, and found it relieved hypersensitivity associated with persistent pain states to the same extend as global deletion of *Fkbp5* (6, 7). Here, we have used genetic and pharmacological blockade of FKBP51 in a pre-clinical model of persistent joint pain and report that modulation of the stress axis through FKBP51 inhibition improves both the sensory and affective component of persistent pain, but in a time dependent manner. Crucially, acute inhibition of the stress axis during disease onset provided permanent relief of both pain and affective symptoms and dampened the expression of *Naaa*, a crucial driver of the transition from acute to chronic pain.

Results

All statistical tests and full analysis results are presented in **Supplementary Table S1+S2**.

We first established the full behavioural phenotype of male and female mice with joint pain induced by the injection of monoiodoacetate (MIA) in the knee joint, up to 6 months after MIA injection. Mechanical allodynia, assessed traditionally by application of manual Von Frey filaments, rapidly developed in both sexes and was maintained throughout the 6-month period (Fig.1.A1; Table S1 for full statistical report). There were no obvious sex differences at any specific time point. However, when looking at single weighted average for each animal for the period (Fig.1.A2), there was a strong trend for effect of sex (P=0.0632), suggesting that the female MIA-group were slightly more sensitive than males across the 6-month experiment. Similarly, both males and females developed immediate and robust changes in weight bearing profile, as they shifted their weight to the contralateral hind leg in the static weight bearing test (Fig.1B1,2), with greater impairment for the females (Fig.1.B1,2). Impairment in weight bearing was greatest in the first 3 weeks after MIA injection, after which it stabilised. We also looked at the impact of the joint disease on bone volume, as a surrogate measure of bone deformation, and found that the injection of MIA had led to a full remodelling of the bone by 6 months, in both males and females (Fig.1C).

We then looked at the affective aspect of the pain experience. First, we compared stress hormone levels between injured and control males and found no significant difference either at 48h or 30 days after MIA injection, suggesting that stress-hormone increase, if any, would be short-lived (Fig.S1,A). Next, we looked at affective behaviour and found that the duration of affective-motivational response to Von Frey stimulation (intensity: Low = 0.04g, Medium = 0.16g, High = 1.0g) was increased by MIA, especially in the first 3 weeks after injection (Fig.1D1,2, Fig. S1, B1,2 and C1,2). There was a greater affective-motivational behaviour in females than in males in this early phase of the disease, as demonstrated by significant interactions between sex and injury (and significant effect of sex for the highest filaments, Fig.S1C). Since most animals had returned to baseline for this specific outcome measure by 6 weeks post MIA injection, this behavioural assessment was discontinued to reduce burden on the animals.

Overall, these results suggested that the sensory impact of the MIA injection was almost immediately stable, while the functional and affective impairments peaked during the first 3 weeks of the disease state.

We next looked at depressive-like behaviour and found that it developed in both male and female mice from 90 days post MIA injection and lasted for at least 6 months (Fig.1E1,2). We had previously reported that, as for humans, depressive-like behaviour does not develop in all animals suffering from chronic joint pain (5). We therefore used an individual profiling approach to assess individual outcomes. Affected animals were defined as those responding one standard deviation or more from the average performance of the control group (22, 23). This approach confirmed that not all animals displayed comorbidities, with the number of females displaying depressive-like behavior increasing as the pain state was maintained, while males reached a peak at 4 months (Table1).

When we looked at anxiety-like behaviour, we found that both male and female mice displayed an anxious phenotype at 3 months and with a clear trend at 6 months, with no obvious sex differences (Fig.1F1-3). Interestingly, both anxiety- and depressive-like behaviour correlated with mechanical allodynia both at 3 and 6 months across sexes (Fig.1G1,2). In line with our previous work establishing that early pain-related burden may serve as a predictor of later disease outcome (5), we also found that the early mechanical allodynia significantly correlated with the level of anhedonia and mechanical allodynia at 6 months (Fig.1H1, 1H2). Only a trend was seen for anxiety-like behaviour (Fig.S1D). Similar findings were detected for correlation with the 3-month time point, and when using WB as a predictor (See Table S3 for all prediction correlations).

Finally, we characterised the sleep and activity patterns of female and male mice for up to 6 months after MIA injection. Here, mice were single housed for a maximum of 2 weeks at a time for monitoring of activity, as before (5). There were no obvious differences in the sleep and activity patterns between 8-week old male and female mice before MIA injection, as shown by 24h activity plots (Fig.2A,B; Fig.S2). MIA had a significant impact on sleep and activity patterns in the very early stages of the joint pain state, specifically during ZT14 and ZT1. In particular, there was a significant increase in the proportion of time spent sleeping in that period, along with a significant reduction in activity in both male and female mice (Fig.2C,D). There was a noticeable difference in behaviour according to sex as injured females could maintain activity levels for longer than injured male mice that showed earlier activity deficit and increased sleep after injury (Fig.2C,D, ZT14 to ZT1: significant time x injury x sex interactions; Table S1). Summary statistics of circadian disruption confirmed these observations and indicated that injured mice were less

able to sustain long bouts of activity (Fig.2E1) and had increased sleep in the dark-phase (Fig.2E2) and decreased sleep in light-phase (Fig.2E3). From one-month post injury, differences between injured and non-injured mice were subtle, while sex differences became more obvious as mice aged (Fig.S3, S4).

Following the full characterisation of mice behaviour after MIA injection, we asked whether the inhibition of the stress driver FKBP51 could reduce the pain phenotype beyond its documented effects on mechanical hypersensitivity (6–8, 24). First, we used *Fkbp5* global KO mice, as before (6, 7). We had previously shown that both male and female mice with the gene *Fkbp5* globally deleted showed reduced mechanical hypersensitivity to persistent pain of various origins (6, 7). Following the injection of MIA into the knee joint, both male and female *Fkbp5* KO displayed mechanical allodynia and weight bearing deficit that lasted for 6 months but of significantly reduced magnitude compared with control WT mice (Fig.3A1,2; B1,2). There were no sex*genotype-interaction affecting the sensory and functional outcomes, suggesting that the *Fkbp5* deletion did not affect the two sexes differently. However, as established in the characterisation experiment (Fig.1), females generally displayed higher functional deficits across genotype, resulting in a sex-effect in the overall statistical analysis for this dataset (Table S1). Importantly, the deletion of *Fkbp5* had no impact on MIA-induced bone deformation when corrected for body weight, which was an important correction due to the leaner phenotype of the KO mice (20, 25) (Fig.3C, Fig.S5A1,2, B). We next investigated emotional behaviour and observed that *Fkbp5* deletion reduced the MIA-induced development of depressive-like behaviour across sexes (Fig.3D) but had a milder impact on anxiety-like behaviour, as seen by the results of the OFT (Fig.3E, Table 2). While these results might have been confounded by increased locomotion in the KO mice (Fig.S5C), the mild differences in anxiety-like behaviour between KO and WT mice after MIA were confirmed by EPM. (Fig.S5D). Using our behavioural profiling, approach, we confirmed that more KO than WT mice were resilient to MIA-induced depressive-like behaviour (Table 2). We also confirmed the lack of differences in anxious phenotype between genotypes (Table 2).

Overall, there was no significant correlation across sex and genotype between sensory and emotional outcomes, when compared at a given time point (Fig.3F1,2). Moreover, while early mechanical allodynia was a significant predictor of late pain sensitivity, it could not predict anxiety- and depressive-like behavior at 6 months (Fig 3G),

although there were trends at 3 months for the depressive-like behavior (Table S3). These results suggested that *Fkbp5* knockdown disrupted the relationship between pain burden and emotional comorbidities, likely due to the reported impact of *Fkbp5* deletion of anxiety-like behaviour independently from the hypersensitive state (25, 26).

We also characterised the impact of *Fkbp5* knockdown on joint pain-induced disruption of sleep and activity patterns. While there were no obvious sex and genotype differences in 8-week-old mice before the injection of MIA (Fig.4A,B,S6), *Fkbp5* KO male and female mice showed increased activity between ZT14 and ZT1 after MIA, when compared with WT mice (Fig.4C,D). These results suggested that the deletion of *Fkbp5* provided some protection to the injury-induced disruption to sleep and activity patterns. Moreover, MIA-induced disruption in a number of summary statistics of circadian activity (Fig.2E) were resolved by *Fkbp5* knockdown, including in long-bouts of activity (Fig.4,F). As mice aged, and at a time where the effects of the injury were no longer obvious in WT mice (Fig.S3,4), genotype and sex differences grew stronger. In particular, the KO females were more active in the dark phase and slept less in the light phase than their wild–type counterparts (Fig.S7, S8). Overall, these results suggested that the impact of global *Fkbp5* knockdown on sleep and activity patterns went beyond the recovery of MIA-induced disruption.

As global deletion of *Fkbp5* led to a substantial improvement of the overall pain experience of mice with joint pain but significant, albeit mild, non-injury related changes to circadian patterns, we next asked whether this could also be achieved through pharmacological blockade of the protein FKBP51. For this, we used the unique FKBP51 inhibitor, SAFit2, as before (6, 7). First, SAFit2-VPG, a formulation that allows slow release of the inhibitor for 7 days through encapsulation in a phospholipid gel was administered 2 weeks after the MIA injection. We chose this time as we had shown it had a significant impact on mechanical thresholds in models of ankle joint inflammation and neuropathic pain (6). As before, we found that SAFit2-VPG attenuated the MIA-induced drop in mechanical thresholds, with mechanical thresholds nearly returning to baseline (Fig.S9A). Weight bearing deficit were equally improved (Fig.S9B). Next, we delayed the administration of SAFit2-VPG to 1 month after the injection of MIA and we extended the duration of FKBP51 inhibition to 3 weeks. This was achieved by weekly injection of SAFit2-VPG for 3 consecutive weeks. SAFit2-VPG significantly increased the mechanical thresholds that had been reduced following

MIA injection (Fig.5A1,2) and promoted the return to baseline of the weight bearing profiles (Fig.5B1,2). We next administered SAFit2-VPG during the 2- to 3-month period after MIA, which corresponds to the time that long-term affective disorders such as depression-like behaviour and anxiety-like behaviour manifest (Fig.1E,F). SAFit2-VPG administered 2 months after MIA injection had a significant effect on mechanical threshold and weight bearing deficit in both male and female mice (Fig.5C,D). SAFit2-VPG also delayed the development of depressive-like behaviour (Fig.5E). Unexpectedly, SAFit2-VPG had no impact on anxiety-like behaviour as injured animals that received SAFit2-VPG showed similar patterns of anxiety-like behaviour as vehicle treated injured mice (Fig.5F, Fig S9C-D), nor did it affect locomotor activity (Fig S9E) or body-weight (Fig S9F). The stronger effect of SAFit2-VPG on depressive-like behaviour was also observed using individual animal profiling (Table 3).

Furthermore, at 3 months, while SAFit2 was still active, there were significant correlations between improvement of both functional and sensory outcome measures and the antidepressant effects (Fig 5G). While the pain relief effects quickly normalized when treatment was discontinued, the antidepressant effects were maintained for longer, with significant predictive correlations between the pain-related outcomes measured during the active phase of SAFit2 and the depressive-like behavior at 3 weeks after treatment-end (Fig 5H) but not 6 weeks after treatment-end (Fig 5I). As we were surprised by the absence of effect of SAFit2-VPG on anxiety-like behaviour in injured mice, we explored the effect of prolonged SAFit2-VPG on naïve mice. When SAFit2-VPG was given to naïve mice as a 1-month treatment, SAFit2 alone induced the development of anxiety-like behaviour (Fig.S10A), as indicated by the reduced time spent in the middle of the arena in the OFT. This is likely why SAFit2 could not prevent MIA-induced anxiety-like behaviour (Fig.5E). Finally, SAFit2 had no effect on mechanical threshold (Fig.S10B) or depressive-like behaviour in naïve mice (Fig.S10C-D).

As the recovery of the MIA-induced allodynia and weight bearing deficit seem to reduce as the administration of SAFit2 was delayed, we next explored the effect of early blockade of FKBP51 during the onset of the pain state. When SAFit2-VPG was administered before the initiation of the pain state, we observed a reduction in MIA-induced allodynia (Fig.6A1,2) and both static and dynamic weight bearing deficit (Fig.6B-C, Fig S11A-C) of similar effect size than that seen when SAFit2-VPG was given 2 weeks and 4 weeks after MIA (Fig.6D-E). Remarkably, for up to 6

months after injury, mechanical threshold and weight bearing never reached the levels seen in vehicle treated MIA animals, despite SAFit2 being only active for up to 10 days after MIA injection (Fig.6A,B). The early SAFit2 treatment resulted in a sensory profile that was similar to that of the *Fkbp5* KO mice (Fig.3A,B). Importantly, early SAFit2 treatment did not exacerbate the degradation of the knee bone induced by MIA (Fig.6F), despite the increased load on the joint, suggested by the weightbearing measure (Fig 6B).

We also investigated the impact of early SAFit2 administration on affective behaviours. Early FKBP51 inhibition reduced affective responses to Von Frey filament applications (Fig.7A, Fig.S12,A-B) and brush-induced allodynia (Fig.S12C) early after the initiation of the pain state. Assessing behavioural changes beyond the active phase of SAFit2, *i.e.* after 2 weeks post MIA injection, we found that the early and acute treatment prevented both depressive- (Fig.7B), and anxiety-like behaviour (Fig.7C, Fig.S12D) at 3 months after injury. Specifically, the development of depression-like behaviour in male mice was delayed by at least 3 months and never occurred in female mice (Fig.7B, Table 4). Finally, the early SAFit2 administration did not lead to any change in body weight compared with vehicle treated mice (Fig.S12E) and had no impact on distance travelled as measured in the OFT (Fig.S12F).

Across sexes, there were significant correlations between pain-related outcomes (allodynia and weight bearing) and both anxiety- and depressive-like behaviour at 3months. Only the correlation between pain-related outcomes and depressive-like behaviour remained at 4.5months, and all correlations were lost at 6 months (Fig.7D). The impact of SAFit2 on the late pain experience, *i.e.* on both pain-related outcomes and emotional comorbidities, seemed to be a direct outcome of its early impact on the pain-related measures, as there was a strong predictive correlation between the pain-related measures in the first two weeks, and the later development of pain-related (Table S3), anxiety- (Fig.7E1-2) and depressive-like behaviour (Fig.7F1-2). The predictive quality was significant for all outcomes at 3 months, for both pain-related and depressive-like behaviour at 4.5 months, and only for mechanical allodynia at 6 months (Table S3).

The impact of SAFit2 inhibition on circadian patterns was also investigated. Exposure to SAFit2-VPG alone had a significant impact on circadian patterns (Fig.8A,B). This was not surprising as we had already observed an increase

in anxiety-like behaviour when SAFit2-VPG was administered for one month in naïve mice (Fig.S10A). Specifically, there was a significant and sex-dependent effect of SAFit2-VPG on the sleeping and activity patterns between ZT14 and ZT1. Notably, there was an increase in activity in female mice and a decrease in male mice during their active phase (ZT14 to ZT1, sex*treatment interactions; Fig.8B, Table S1). However, there were no significant differences in the summary parameters of circadian disruption between SAFit2-VPG and vehicle treated mice, suggesting that the SAFit2-induced differences may be considered somewhat mild (Fig.S13). After the initiation of the pain state, early SAFit2-VPG treated mice slept less and were more active than vehicle treated control mice (Fig.8C,D, Table S1), suggesting that SAFit2-VPG had a protective effect on the MIA-induced changes in sleep and activity patterns. However, the impact of FKBP51 inhibition on summary parameters of circadian disruption were milder and rarely reached significance, likely due to the significant sex differences increasing the variability in the data (Fig.8E). As we had observed previously, as mice aged, sex differences became more obvious, with mild effect of the early FKBP51 inhibition (Fig.S14). Overall, the impact of early FKBP51 pharmacological inhibition on circadian patterns were milder than the global knock-down of *Fkbp5* but still improved some of the MIA-induced deficits.

Our findings demonstrated that early and acute FKBP51 inhibition during MIA onset provides long-term pain relief that outlasts the active phase of the pharmacological compound, while FKBP51 inhibition from 2 weeks after the initiation of the pain state only provides temporary pain relief. To try and identify the mechanisms underlying these differences, we used an RNA sequencing approach. All mice received an MIA injection into the knee joint but one experimental group received SAFit2-VPG or vehicle during the initiation phase of the pain state (early treatment), while the second group received SAFit2-VPG or vehicle once the pain state was fully established (late treatment). As before, the mechanical threshold of animals that received SAFit2-VPG early remained greater than that of vehicle treated control animals beyond the active phase of SAFit2-VPG (Fig.9A). Tissue was collected on day 30 after the MIA injection, *i.e.* after the active phase of SAFit2-VPG for the early treatment group but during the active phase for the late treatment group. Overall, there was no difference between the mechanical threshold of early and late treated mice at the time of tissue collection (Fig.9A). However, the weight bearing/gait improvement provided by the early treatment was greater than that seen in the late treated group (Fig.9B, S15A-D). Corticosterone levels were reduced by SAFit2-VPG (Fig.9C) and correlated with Von Frey thresholds at the time of dissection (Fig.9D).

We next looked at gene expression levels in the ipsilateral quadrant of the spinal cord of injured mice using RNA sequencing. Our aim was to identify genes uniquely differentially expressed by the early SAFit2 treatment *vs* late SAFit2 treatment, as we had hypothesized that these would underlie the mechanisms of long-term pain relief provided by the early treatment.

We first asked what the overall effect of SAFit2-VPG treatment was, combining the early and the late groups. Linear regression modelling of the main treatment effect detected 1185 genes that were differentially regulated (nominal $P<0.05$) by SAFit2-VPG when compared with vehicle. Inspection of these differentially expressed genes (DEGs) using principal component analysis revealed sub-clusters within the second principal component of SAFit2-VPG-treated groups exposed at the early *vs* late time points which was not present in vehicle-treated groups (Fig.9E). Out of the 1185 treatment DEGs, 311 were up-regulated and 534 were downregulated by SAFit2-VPG with a cut-off fold-change of 1.2 (Fig.9F). Interestingly, *Fkbp5* was one of the 311 up-regulated DEGs (Fig.9G).

We then characterised the signalling pathways modified by SAFit2-VPG specifically while the drug was still active, focusing on the late treatment group. A nested analysis ($Late_{SAFit2}$ *vs* $Late_{Vehicle}$) revealed that 757 genes were significantly differentially expressed by the late SAFit2 treatment (adjusted FDR $P<0.05$), with 332 downregulated and 425 upregulated genes (Fig.9H). We next hypothesized that if the DEGs were functionally relevant to the reduced mechanical threshold observed in $Late_{SAFit2}$ treated mice, their expression level would correlate with the mechanical thresholds measured before dissection. Using Pearson's correlation analysis with Bonferroni correction, we found that the expression levels of 702 DEGs correlated with the mechanical threshold (average day 27 to day 30). Out of these 702 DEGs, 434 were not included in the 1185 identified main treatment DEGs (Fig.10A), suggesting that these genes were transiently modulated by SAFit2-VPG treatment. Further gene ontology (GO) analysis indicated that the 434 identified DEGs contributed to various biological processes including energy metabolism, cell structure regulation, neuronal development, RNA processing, protein transport and sensory perception (Fig.10B). A number of downregulated DEGs stood out, as they had been previously involved with nociceptive signalling and their inhibition was found to reduce hypersensitivity, including: *Shank3,* linked to autism spectrum disorder and pain signalling (27, 28) (Fig.11A), *Hdac5,* the gene encoding for the histone deacetylase 5 (29) (Fig.11B), *Faah,*

encoding the fatty acid amide hydrolase, the enzyme that hydrolyzes the endocannabinoid anandamide and associated with pain insensitivity in humans (30, 31) (Fig.11C) and *Src,* encoding the non-receptor tyrosine kinase (32, 33) (Fig.11D). We also observed that late SAFit2-VPG treatment promoted the expression of the gene encoding the Phosphatase and Tensin Homolog, *Pten,* known to protect from neuropathic pain (34) (Fig.11E). Finally, SAFit2 was likely to promote NF-KB signalling through the inhibition of the NFKB inhibitor *Nfkbib* (Fig.11F). However, a number of pain related genes were also regulated in a direction that could suggest enhancement of hypersensitive state (Fig.S16).

We next investigated genes similarly regulated by early and late SAFit2 treatment, *i.e.* DEGs that were at the intersection of the 2 analyses (SAFit2 overall effect-n=1185 and late treatment nested analysis -n=757: n=268 DEGs, Fig.10A). Only one of those genes had expression levels that correlated with mechanical hypersensitivity (*Eri1*, a protein-coding gene that is involved in a variety of RNA metabolic pathways Fig.10A). We also identified several DEGs involved with nociceptive signalling (Fig.S17). However, the regulation of these genes alone could not underpin the long-term impact of early SAFit2 treatment as animals that received late SAFit2 treatment were expected to return to a fully hypersensitive state after the drug's active phase.

To elucidate the mechanisms of pain relief provided by early SAFit2 treatment, we first tried and identified DEGs modified by early SAFit2 administration by drawing contrasts between $Early_{SAFit2}$ and $Early_{Vehicle}$ treated mice from the nested approach. However, there were no DEGs with FDR corrected $P<0.05$. To identify genes most likely to drive the mechanisms underlying the long-term relief provided by early SAFit2 treatment, we first focused on the 1185 DEGs that were not modified by the late treatment alone (*i.e.* 1185 Δ 757) (n=893 DEGs; Fig.10A). GO analysis of this subset of genes revealed that these were mainly related to cilia and motility-related processes, as well as cytoskeleton organisation (Fig.S18). We further refined our identification of genes likely to be modulated by early SAFit treatment by comparing the change in expression (SAFit2 Δ Vehicle) between early and late treatments. Using this approach, we identified 202 annotated DEGs that showed greater change in expression when the SAFit2 treatment was administered early (Fig.10A). While most of these genes were still related to cilium movement and assembly (Fig.12A), several genes had previously been shown to promote a pain phenotype (Fig.12B) and were

reduced following early SAFit2 treatment. These included the preproenkephalin gene *Penk*, which encodes precursors to the endogenous opioid peptides enkephalins, *Enkur,* which encodes the protein enkurin, known to interact with TRPC channels, as well as *Aplnr,* which encodes the apelin receptor (or angiotensin II receptor-like 1). The *Naaa* gene, which encodes the enzyme N-acylethanolamine acid amidase, also belonged to this subset of genes and crucially had been previously linked to transition from acute to chronic pain (35).

Altogether, our RNAseq analysis suggested that early SAFit2 treatment may induce lasting changes in gene expression at spinal cord levels that are not observed with late treatment, potentially contributing to sustained pain relief.

Discussion

Our study provides a comprehensive analysis of the behavioural and molecular impact of the modulation of the stress axis through inhibition of the stress regulator FKBP51 during joint pain induced by the injection of MIA into the knee joint.

We have used the MIA model of knee OA (36–39), a model with strong translational value that induces rapid disease progression, is responsive to conventional pain-relieving therapies (38, 40) and produces histological alterations similar to those found in clinical histopathology (41, 42). OA is the most common joint disease (43, 44) and is accompanied by clinically significant anxiety and/or depression in at least 41% of patients (45), with anxiety and depression positively correlated with pain severity (46). Here, knee injection of MIA induced a persistent hypersensitive state that lasted at least 6 months, in both male and female mice, and was accompanied by emotional comorbidities, as reported by patients. While the hypersensitive state and functional deficit developed in all animals immediately after the injection of MIA, the development of emotional comorbidities, namely anxiety- and depressive-like behaviour, was more progressive, emerging from 3 months after disease onset, and only present in a subset of animals. This aligns with the clinical observations and also previous research suggesting that emotional comorbidities have delayed onset compared with the hypersensitivity-related measures (47, 48).

Small but significant sex differences were observed in mechanical hypersensitivity, affective responses and functional deficit, with females being more sensitive to MIA, despite adjusting the dose of MIA to animal weight. Sex differences in emotional comorbidities, if any, seemed more complex and may indicate different time course of development. Regardless of these mild sex differences, both the sensory and functional aspects of joint pain in the late stage of the disease correlated with emotional comorbidities across sexes and more importantly early sensory and functional measures correlated with late pain intensity and depressive-like behaviors. These results supported our previous findings in male mice indicating that early pain burden could serve as a predictor of long-term emotional outcomes (5). Further strengthening the idea that the early pain experience could dictate the late emotional outcomes, the greatest impact of FKBP51 inhibition on the overall pain experience was seen when the inhibition occurred during the onset of the disease state. Indeed, blocking FKBP51 in the early stages delayed or

prevented, the emergence of an anhedonic state. Similar beneficial effects were also seen on anxiety-like behavior. Such impact of early FKBP51 inhibition had been suggested by a previous study looking at post-traumatic stress induced pain (8). In our study, delayed treatment, starting anytime from 2 weeks to 2 months after initiation of the pain state, still yielded beneficial effects, but these were only transient. It's important to note that in the MIA model, most pain-like behaviours are most severe during the early stages of the disease. Therefore, our observations with the early treatment may be related to the reduction of peak pain levels, rather than the timing of the intervention.

Overall, our results supported our original hypothesis that manipulation of the stress axis through FKBP51 inhibition, regardless of the timing of the treatment, improves both the sensory and emotional impact of persistent pain. When FKBP51 inhibition was provided at 2-3 months, in the phase leading up to the typical onset of comorbidity, depressive-like behavior was successfully prevented, with prolonged beneficial effects compared with sensory impact, as seen by improved mood behaviour lasting for 3 additional weeks after analgesic effects disappeared. This suggests that onset of depressive comorbidity is delayed and potentially secondary to sensory and functional effects, as reported by others (49). It is noteworthy that long-term FKBP51 blockade *(i.e.* for 4 weeks) in injured mice had no impact on anxiety-like behaviour. This may not be surprising as the long-term SAFit2-VPG treatment in naïve mice caused anxiety-like behavior, unlike acute treatment that provides anxiolytic effects in the context of stress exposure (13, 14). The secondary anxiolytic effects to pain relief may therefore have been neutralised by the anxiogenic effects observed after long term use of the compound in un-injured conditions. Nonetheless, as SAFit2 consistently improved both the sensory aspect and depressive-like behaviour, without worsening the anxiety-like behaviour in injured mice, our results suggest that FKBP51 inhibition through long-term SAFit2 exposure could be effective for long-term chronic pain management.

Our home cage activity recordings of both naïve *Fkbp5* KO, and naïve WT mice treated with SAFit2-VPG brought a different perspective. Indeed, in both cases, manipulation of the stress axis led to significant impacts on circadian patterns, more obvious in female mice. These changes were longer-lasting than the MIA-induced changes, which did not persist beyond 2 weeks, as it had been previously reported with other on-going pain metrics (50). While previous studies had found no impact of FKBP51 deletion on circadian rhythms when assessing wheel-running

activity (51), FKBP51 had been identified as a target for stress-induced sleep disorders, and its deletion promoted better sleep in disease state (15). Therefore, FKBP51-inhibition-associated changes could be seen as protective in the early stages of the MIA-induced joint pain. Nonetheless, in our study, these changes outlasted the short-lived MIA-induced changes in the KO mice without obvious benefit on sleep quality. However, when SAFit2-VPG was administered acutely only during the onset of the disease, there were no persistent impact of SAFit2-VPG treatment on sleep and activity patterns, suggesting stronger therapeutic benefit of this approach.

Overall, targeting the stress axis by acute pharmacological inhibition of FKBP51 at the onset of the disease provided effective, long-lasting pain relief, which continued beyond the drug's active phase without obvious side-effects. We wanted to elucidate the mechanisms underlying these observations and investigated gene expression changes induced by SAFit2 treatment given both in the early and the maintenance phase of the pain state. We focused on the spinal cord, specifically the ipsilateral quadrant of the superficial dorsal horn, as our original work suggested that FKBP51 drives chronic pain through spinal mechanisms (7). Genes uniquely modified by active SAFit2, and therefore transiently modulated by FKBP51 modulation, often correlated with mechanical hypersensitivity, suggesting some potential functional relevance. These belonged to various biological processes including sensory perception and a number had been previously involved with nociceptive signalling including *Shank3*, *Faah*, *Pten*, *Hdac5* and *Src*. *Src* was particularly relevant as morphine induced hypersensitivity is accompanied by an increase in *Src* at spinal cord level and can be blocked by *Src* inihibition (33). Surprisingly, we did not observe changes in glucocorticoid signalling, despite SAFit2's impact on cortisol levels. However, the effect of SAFit2 on cortisol was relatively mild, and previous studies have also reported no significant influence of SAFit2 on stress hormone levels (52). On the other hand, we observed a decrease in *Nfkbib* expression, indicating that SAFit2 may promote NF-κβ signalling. The role of FKBP51 in this context is complex, with previous studies suggesting that it could both inhibit and facilitate NF-κβ signalling in various cell types (53).

When we tried to identify genes that were modulated by the early SAFit2 treatment, we found that no gene passed our threshold for significance (FDR adjusted $P<0.05$) and expression level (1.2-fold), suggesting a very small effect size. Nonetheless, combining early and late treatment, we found that several DEGs were modulated by SAFit2

overall and not late SAFit2-VPG treatment alone, suggesting that the significance for several DEGs may have been driven by changes following the early treatment. Looking specifically at the DEGs showing greater changes after early SAFit2-VPG treatment, we found that most of these genes were related to cilium movement and assembly. The primary cilium is an organelle crucial in cellular signalling that projects from the cell surface of most post-mitotic cells including neurones in the CNS. The role of primary cilia in spinal neurones has been rarely studied and cilia related genes have yet to be associated with spinal nociceptive signalling. However, primary cilia in large and small neurones of the dorsal horn of the spinal cord have been described (54). Moreover, primary cilia serve as a key hub of transmission for Sonic Hedgehog (Shh) signalling which has a significant role in pain modulation and their role in peripheral signalling in nociceptors has recently been highlighted (55). Our findings suggest that long-term re-organisation of spinal cilia following early SAFit2 treatment may provide long-term pain relief. Interestingly, it was recently suggested that the μ- opioid receptor selectively localize to primary cilia in the mouse CNS (56), which may contribute to the phenotype observed in early treated mice. We also found that early SAFit2-VPG treatment persistently reduced the expression of *Penk*, the gene encoding for preproenkephalin, while *Penk* derived peptides have been shown to delay recovery from inflammatory hypersensitivity (57). Finally, one non cilium related DEG particularly stood out, the *Naaa* gene which encodes the enzyme N-acylethanolamine acid amidase (NAAA). NAAA has been identified as a crucial control point in the progression to pain chronicity and inhibition of NAAA in the spinal cord after peripheral injury during a 72h time window can prevent chronic pain (35). Here, we found that SAFit2-VPG treatment in a similar time window after MIA injection led to a long-lasting downregulation of *Naaa* compared with controls and mice that received SAFit2-VPG later.

In conclusion, our findings underscore the therapeutic potential of targeting FKBP51 in the early stages of osteoarthritis to not only manage pain but also mitigate the development of emotional comorbidities. The prolonged pain relief observed with early FKBP51 inhibition, alongside its impact on gene pathways associated with nociceptive signalling and primary cilia function, suggests a novel approach to chronic pain management. However, given the disruption of circadian rhythms observed with long-term inhibition, future research should focus on optimizing treatment timing and exploring the broader implications of FKBP51 inhibition on sleep and emotional health. Investigating the precise molecular mechanisms underlying cilia function and the role of NAAA in chronic

pain progression will be crucial for refining therapeutic strategies and ensuring long-term efficacy without adverse effects.

Methods

Animals and housing;

Male and female mice (C57Bl/6J from Charles River, UK) arrived at our facility at 8 weeks of age, and were left to acclimatize for at least 7 days before experiments started. *Fkbp51* KO colony was maintained at UCL breeding +/- animals together, and experiments were started when they were 8-10 weeks old. *Fkbp5* KO and their WT littermates were previously obtained from FKBP51 heterozygous from C.A. Dickey's group (University of South Florida, USA). These mice were from mixed genetic background, C57Bl/6J and Swiss Webster. All animals were kept in groups of 2-4 in a temperature-controlled (20±1°C) environment in Individual Ventilated Cages-cages (SealSafe Plus GM500, Tecniplast, 39*19*16cm); equipped with sawdust (Lignocel Select fine), nesting material (Datesand Cocoons), wooden chew stick (LBS Small Aspen chewstick) and cardboard tunnels for shelter and handling (LBS Standard Fun tunnel); light-dark cycle of 12 hours (gradual lights on between 7-8a.m. and off between 7-8p.m; in our sleep studies, ZT0=7am, ZT12=7pm); and ad libitum provision of food and water (Teklad global 2018 diet). The only exception to these housing-conditions was during the sleep/activity-recordings, where animals were single-housed in open wire top M1 mouse cage (North Kent Plastic Cages, 45*28*13cm) without tunnels for shelter. All experiments were carried out under the Home Office License P8F6ECC28, ARRIVE guidelines were followed, and all efforts were made to minimize animal suffering and to reduce the number of animals used (UK Animal Act, 1986).

Genotyping

Genotyping was performed as previously described (6, 7). DNA was extracted from a small portion of ear tissue and the following primers were used for the PCR: forward primer (for WT and 51KO): AAAGGACAATGACTACTGATGAGG; reverse WT primer: AAGGAGGGGTTCTTTTGAGG; reverse 51KO primer: GTTGCACCACAGATGAAACG. Samples from WT animals showed a single PCR product of 363bp; samples from KO animals showed a single PCR product of 510bp and samples from HET animals would present both bands.

Compound preparation and administration:

SAFit2 was synthesised as before (21), encapsulated in Vesicular Phospholipid Gel (VPG; 50% (m/m) egg lecithin containing at least 80% phosphatidylcholine in 10 mM phosphate-buffered saline (PBS) pH 7.4; used at 10 mL/kg or 100 mg/kg) in a dose of 10mg/ml. Vesicular phospholipid gels (with and without SAFit2) were prepared by a dual asymmetric centrifugation (DAC) technique as described below. SAFit2-VPG was always provided subcutaneously under anaesthesia in a dose of 1mg/10g, providing approximately 7 days of slow release (6).

Preparation of vesicular phospholipid gels by dual asymmetric centrifugation

Vesicular phospholipid gels with a phospholipid amount of 50% (m/m) were prepared by DAC. To encapsulate the poorly water-soluble SAFit2 into the formulation by a direct incorporation method, the accurately weighted phospholipid was solved in ethanol (100%) and SAFit2 stock solution (20.0 mg/mL in 100% ethanol) was added in the desired amount to the phospholipid solution. The ethanol was evaporated for 2 days in a vacuum drying oven at a temperature of 25°C and a pressure of 10 mbar. Then, the solid mixture was hydrated with the accurate amount of 10 mM PBS buffer pH 7.4 and homogenized by a DAC (Speedmixer DAC 150.1 FVZ; Hauschild GmbH &Co. KG, Hamm, Germany).

Dual asymmetric centrifugation is a double centrifugation technique which is perfectly suited for the mixing of highly viscous formulations and has been used in the past to prepare liposomes and fat emulsions. Its application to manufacture VPGs has been first described by Massing et al. in 2008 (58). In this technique, the container is not only spun around the commonly known centrifugation axis in the middle of the centrifuge but also around a second axis in the middle of the container. Because of the 2 counterrotating movements, high shearing forces and a homogenous mixture of the components are achieved.

For homogenization of the phospholipids and buffer in our study, a process speed of 3500 rpm was used. A custom-made cooling system was installed to prevent the material from heating during the continuous mixing over 45 minutes. The final amount of SAFit2 in the formulation was 10 mg/g. Then, the solid mixture was hydrated with the accurate amount of 10 mM PBS buffer pH 7.4 and homogenized by a DAC (Speedmixer DAC 150.1 FVZ; Hauschild GmbH &Co. KG, Hamm, Germany).

The described manufacture process was used for the preparation of a second VPG formulation without the addition of SAFit2 stock solution as a control formulation (Vehicle).

Study design;

The study was divided in a series of experiments, each with different constellations of tests and duration, designed to answer specific questions (Table 5). All behavioral experiments generally included assessment of most behavioral outcomes in the same set of animals, except the activity/sleep assessment, which was recorded in a separate set of animals, due to the need for single-housing during these experiments.

Animals were allocated into groups using block randomisation, securing equal representation of treatment-groups in each cage, to minimise potential confounders related to housing/cage. Overall, each study included equal numbers of animals in each group, but due to the toxic nature of the MIA-chemical, a few animals were lost during model-induction in some experiments. Equally, due to the long-term nature of the experiments, some animals were lost at different stages of the experiment due to other accidental losses not related to the experiment, like fighting wounds or dermatitis. Additionally, two animals were excluded from the weightbearing-assessments in Fig 5B and 5D before treatment-initiation, as they were not compliant in the WB-assessment. Besides these few exceptions, no animals were excluded from experiments or the following analysis. And due to these variations, N-numbers were not always equal, and at times defined in a range (full overview of numbers in each study, see **Table S1+2**). A total of 334 mice were used for these studies.

Key outcomes, like mechanical sensitivity and weight bearing, was assessed frequently through most experiments, while assessment of catwalk, anxiety- and depressive-like behavior were only assessed on selected timepoints, based on previous experience (5), the characterization study (Fig 1) and hypothesis of each individual experiment.

Experimental procedures;

Induction of injury, (MIA); Induction of the Monoiodoacetate Arthritis Model to the knee joint (MIA) was performed similar to previously reported (5, 38). On the day of injection, the monoiodoacetate solution was freshly prepared in sterile saline for injection of 1mg Sodium Iodoacetate (≥98%, Sigma) in 10µl saline (9% NaCl). Animals were anaesthetized in an induction chamber using Isoflurane 2.5% mixed in O_2 at a flowrate of 1.5 L/min, and maintained via facemask at 2.0% during the injection. Anaesthetic dept was confirmed by lack of withdrawal reflex to a pinch to the tail. The animal was then placed on the back in dorsal recumbency, and the fur was shaved in the area around the knee on the left hindleg. The knee was stabilized and fixed in a slightly bent position and the patellar tendon was visualized as a white line below the skin. The injection of 10µl using a 30G insulin-syringe (BD Micro-Fine Plus Demi, 0.3ml (30G) 8mm) was made intraarticularly in the joint space by applying it perpendicularly through the tendon just below the patella, and with as minimal movement as possible. The injection volume was decreased 1-2µl in smaller subjects weighing less than 22g, to account for the smaller joint size and decrease the risk of toxicity when surpassing the maximum volume-capacity of the joint space.

Control animals. Naïve control animals were only exposed to anesthesia.

Behavioural testing;

Behavioural testing was always performed in randomized order and by the same female experimenter, who was blinded to treatment and/or genotype. Animals were always allowed at least 30min of habituation to the testing room prior to behavioural testing. Unless otherwise specified behavioral tests were always performed between 8am and 2pm.

Mechanical allodynia (VF); Low intensity mechanical sensitivity was assessed similar to previously reported in our group (5), using a series of calibrated von Frey monofilaments (0.02; 0.04; 0.07; 0.16; 0.4; 0.6; 1.0) (Ugo Basile SRL, Italy). Animals were placed in Plexiglass chambers, located on an elevated wire grid, and allowed to habituate to the testing environment for at least 60 min prior testing. Once the animals were calm, the plantar surface of the paw was stimulated, starting with a 0.6g filament applied with uniform pressure for 5 seconds. A brisk withdrawal,

stretching or licking of toes, was considered as a positive response, whereupon the next lower-force filament was applied. In the absence of a positive response, the next higher-force filament was applied in the next test. After the first change in response-pattern, suggesting the approximate threshold, additional 4 stimulations were applied; applying the next higher-force filament when no response, and lower-force filament following positive responses. The response pattern determined the constant, *k* (59), and the 50% response threshold was determined using the following equation; 50% threshold (g) = $10^{\log(\text{last filament})+k*0.3}$.

Affective-motivational behavior (AF); in addition to assessing pure reflexive sensory threshold to mechanical stimulation (VF), we also adopted and modified the protocol described (5, 60) to assess the affective responses displayed after stimulation with selected filaments (low; 0.04g, medium; 0.16g, high; 1.0g). The assessment was always performed following the VF-assessment, while the animals were still in the Plexiglas chamber, and following a period of rest. Starting with the low-intensity filament, each filament was applied once for 1sec, and the duration of affective response was recorded as the amount of time, the animal showed conscious attending behavior to the stimulated paw, by licking, biting, lifting or guarding the paw, within 30 seconds after application of the filament. The animal was left to rest for at least 10min before the next higher filament force was applied.

Functional impairment - Weight bearing (WB); To assess the functional impact of the injury the weight bearing distribution was assessed similarly to previously described (5, 61). Hindlimb weight bearing was measured using a Bioseb Incapacitance Test (Bioseb) which measures the weight distribution across the two hindlimbs of a stationary animal. Animals were habituated and trained to become comfortable with the testing paradigm for 5 days prior to induction of the model. Three readings were collected and averaged for each animal, and the weight borne by the ipsilateral limb was expressed as a percentage of the weight borne across both hindlimbs (WB-% = (weight borne on the injured leg/weight borne on both legs) * 100%).

Catwalk gait analysis: Analysis of voluntary movement and gait pattern was performed using the Catwalk® XT 10.0 system (Noldus Information Technology) and based on our previous experience (5, 48). Briefly, green light was internally reflected into a glass plate, on which an enclosed corridor was fixed, with red backlight above the corridor. A video-camera was mounted underneath the setup and recorded the paw prints being lit up by the green light

when paws were in contact with the glass plate as the mouse walked along the corridor. A run was regarded as compliant when the animal entered in one end of the corridor, and moved fluently across the plate towards the other end of the corridor, with a running duration below 12 seconds and a maximum variation below 75%. Three compliant runs were recorded for each animal, with no previous training/habituation or food-deprivation. For outcome-measures like swing-time ratio, contact area and single stance, the data was converted into a ratio between ipsi- and contra-lateral hind-limbs. The parameter "guarding index", was calculated as previously described (62) and the higher guarding index suggests less dynamic weight bearing on the injured leg compared with the non-injured.

Sucrose Preference Test (SPT); In order to assess depressive-like behaviour, the sucrose preference test was included as a measure of anhedonia, as previously described (5). At least 5 days before SPT each home-cage was fitted with two water bottles, in order to have the mice accustomed to drinking from both bottles / sides of the cage. Two days before the SPT test, one of the water-bottles was filled with 1% sucrose solution for approximately 24h, with the two bottles changing side halfway, to allow the mice time to discover the sweet solution, and learn that it may be presented in both sides. No sucrose was provided the last 24 hours before the actual test. For the SPT test, all animals were individually housed in fresh cages in their home-cage environment for 12h overnight, and were given free access to two pre-weighed bottles containing either normal drinking water or 1% sucrose solution. In the morning all bottles were weighed, and mice were placed back together with their cage-mates. This re-introduction released some fighting in especially some of the male cages, and mice were given a night to calm down before the test was repeated overnight with the sucrose bottle presented in the opposite side, to account for potential side-preference, as reported previously in rats (48). No side-preference was detected in the current study, and the sucrose preference % was calculated across the two nights, using the following calculation; SPT% = (sucrose-solution consumed / (total fluid consumption)) * 100%. The sucrose-solution was always prepared fresh before provision at 1% in the normal drinking water, although for one experiment assessing effects of treatment in naive animals (Fig S10) a lower 0.5% solution was also included. As recent meta-analysis suggests food- and water-deprivation to confound the outcome of this assay (63) no water- or food-deprivation was employed in this study.

Elevated Plus Maze (EPM); To assess anxiety-like behaviour an EPM was used as described previously (5, 48) but for these experiments adopted to mice rather than rats. The maze consisted of four arms (35*5 cm) arranged in a cross-like disposition, and 60cm above ground (Ugo Basile SRL, Italy). Two opposite arms were open, and the other two were equipped with 15 cm high walls on each side for enclosement. All were connected by a central 5*5 cm square. The animal was placed in the centre, for free exploration for 5 minutes. Recording was performed by use of a camera placed above the maze, and movement between zones was tracked using EthoVision XT14 (Noldus Information Technology). The maze was wiped with 70% ethanol between each animal to minimize the influence of odours between animals.

Open Field Test (OFT): to assess anxiety-like and locomotor activity, an OFT was used, as previously described (5). The OFT was a circular open arena with grey plastic flooring and blue plastic sides (diameter, 36cm, height 32cm). The arena was evenly illuminated by lighting placed above the arena. A video camera was positioned directly above the arena and connected to a computer performing live-tracking and recording of the behavior using Ethovision XT14. The animal was placed in the middle of the arena and allowed 5 minutes of freely exploration. The proportion of time spent in the centre vs by the edges/walls of the arena, was used as a marker for the anxiety-like behavior (outer zone; 6.7cm along the edge of the arena. Centre zone diameter; 22.6cm).

Sleep/activity-pattern; To measure undisturbed activity in the home-cages, we adopted the approach of Brown et al. (5, 64) using non-invasive passive infrared motion sensors. Animals were single-housed with a 12h light:12h dark cycle. The cages were open with wire tops (M1 mouse cage, North Kent Plastic Cages, floor area: 500cm^2) and a passive infrared (PIR) motion sensor was fitted above the cage. For accurate measurements of activity, the area below the food- and water-hopper was blocked off and tunnels / shelters were removed, allowing the animal to be in the sensors receptive field at all times. Home cage mouse activity was tracked as in Brown et al. (64), with measurements taken every 10 seconds across multi-day periods. As before, sleep was defined as periods in which no activity was measured for 40 seconds or more. Activity and sleep data were smoothed by calculating the mean in 10-minute bins as preliminary experiments demonstrated that this provided a balance between reducing measurement noise and maintaining time series features. Several summary statistics of circadian disruption were

calculated for individual animals across the 5-to-14-day periods (depending on the experiment) and, where appropriate, on each individual day: inter-daily stability, intra-daily variability, light-phase activity, dark-phase sleep, the Lomb-Scargle periodogram, similar to the chi-square periodogram (65).

ELISA

Corticosterone levels were measured as before (6, 7).Immediately upon cervical decapitation, blood was collected in tubes containing trisodium citrate (Paediatric Tube 1.3ml Trisodium citrate 3.2% (9NC), Greiner Bio-One, LTD), gently mixed via inversion and stored on ice. Tubes were centrifuged at 10.000RPM at 4°C for 10min, plasma was collected and stored at -20°C until analysis. Plasma corticosterone was quantified using a commercial ELISA kit for corticosterone (Corticosterone ELISA kit, ab108821, Abcam PLC) according to the manufacturer's instructions.

Sequencing

RNA was extracted from spinal cord lumbar (L4 to L6) quadrants using the Qiagen AllPrep DNA/RNA/miRNA kit as per manufacturer's instructions. RNA was quantified using a Nanodrop 8000 spectrophotometer and RNA integrity was measured using the Agilent 2100 Bioanalyser. All samples passed Quality Control (QC) with RIN scores >7. mRNA libraries were prepared from total RNA using NEBNext Ultra II Directional Library Preparation Kit. Fragmentation of isolated mRNA prior to first strand cDNA synthesis was carried out using incubation conditions recommended by the manufacturer for an insert size of 300bp (94°C for 10 minutes). 13 cycles of PCR were performed for final library amplification. Resulting libraries were quantified using the Qubit 2.0 spectrophotometer and average fragment size assessed using the Agilent 2200 Tapestation. A final sequencing pool was created using equimolar quantities of each sample library. 75bp paired-end reads were generated for each library using the Illumina NextSeq®500 in conjunction with the NextSeq®500 v2 High-output 150-cycle kit to obtain an average of 19.5M read pairs per sample.

Raw paired-end next generation sequencing reads (Illumina HiSeq 2500) were assessed for quality scores and trimmed using a sliding window operation with an average quality score Q > 20. Illumina adapter sequences were also removed. Reference-based alignment was performed using the mouse mm10 genome assembly and

successfully aligned features quantified at the gene-level using featureCounts. Summarised gene counts were transformed into transcripts per million (TPM) to account for biases arising from differing gene lengths (66) and library sizes normalised using trimmed mean of M-values. Gene matrices were filtered by expression using a minimum count > 10 in at least 70% of samples and a minimum overall count > 15 transcripts to remove genes that were either not expressed or lowly expressed among all samples. Differential expression among treatments was established using linear modelling through limma using log2-transformed TPM. Heteroscedasticity of the mean-variance relationship in the latter was removed using limma voom. Genes exceeding a 1.2-fold change in expression and Benjamini-Hochberg (FDR) adjusted p values < 0.05 were considered differentially expressed among groups. When stated explicitly, we additionally performed exploratory analysis on genes with p values exceeding nominal ($p < 0.05$) significance only. Gene overrepresentation tests and gene ontology of significant gene sets were performed using a minimum term size > 2 against the mm10 array background gene set as the reference. Statistical comparisons against the observed *vs* expected gene set ratio were assessed using Fisher's exact tests and corrected using FDR at $P < 0.05$. All annotations were identified using the GO biological process complete database available through PANTHER. GO lists reduced into hierarchical semantically similar terms using ReViGo for plotting. Interrogation of RNA seq data performed in R Studio version 4.3.3 or later.

CT scans;

Following dissection and fixing in 4% paraformaldehyde for 5 days, knee joints were stored in 70% ethanol. Micro-CT analyses were performed using VECTor6CT (MILabs, The Netherlands). Knee joints were imaged using single mouse bed with the following settings: ultra-focus magnification, accurate scan mode, settings default, for a total duration of 6min per CT position. Reconstruction was done using 20voxel size and images were analysed using BoneJ software for bone volume (BV) in region of interests (ROI) of the knee joint. Macroscopic analysis of joints was done using VivoQuant version 4 software (Invicro LLC, Boston, MA, USA).

Statistical analysis;

The experimenter was blinded to genotype and treatment groups until the time of data-analysis. All statistical tests were performed in IBM SPSS Statistic Program (vers 26) or GraphPad Prism (vers 9). Interrogation of RNA seq data

performed in R Studio version 4.3.3 or later. $P<0.05$ was considered statistically significant. Individual animals were considered as experimental unit, and sample-size was based on previous experience, based primarily on securing enough power for the assessment of depressive-like behavior across sex. All statistical tests and significant F-values are reported in supplementary table S1 and S2. Tests for normality of residuals and homogeneity of sample variances confirmed before parametric analysis. Post-hoc analysis was only performed on statistically significant F values. The VF-dataset was log-transformed to ensure a normal distribution, as the von Frey hairs are distributed on an exponential scale. This was similar to previous studies in our group (7), and as demonstrated to make more mathematical and biological sense (67). Most long-term timeline datasets were also converted into weighted average (AVG), either for the entire duration of the experiment, or for selected relevant phases of the experiment, like when a compound was active or the first 2 weeks after model induction.

Study approval: All experiments were carried out under the Home Office License P8F6ECC28, ARRIVE guidelines were followed, and all efforts were made to minimize animal suffering and to reduce the number of animals used (UK Animal Act, 1986)

***Data availability*:** Data can be shared upon request emailed to the corresponding author.

Author contributions: Study conception and experimental designs: SH and SG. **Data collection:** All behavioural studies were done by SH; RF and SG contributed to tissue collection; SG contributed to the recordings of home cage activity. SC acquired joint CT scans. TH synthesised SAFit2. KK prepared the VPG. **Data analysis and interpretation:** SH and SG analysed and interpreted all data. SC contributed to CT scans analysis. SS ran all RNA sequencing analysis and AF contributed to analysis of sleep data specifically. RF and OM provided critical insights throughout the study. **Manuscript preparation**: SH, SS and SG wrote the initial draft of the manuscript. AF, SP provided critical comments and revisions on the draft and all authors read and approved the final manuscript.

Acknowledgments: Funders: This project was funded by a Versus Arthritis grant to SG and FH; Research Award 21972. SS was funded by the Advanced Pain Discovery Platform (MR/W002566/1). SNP is funded by the Biotechnology and Biological Sciences Research Council (BB/X002357/1) and the National Centre for the Replacement, Refinement and Reduction of Animals in Research (NC/V000977/1).

References

1. Radat F, Margot-Duclot A, Attal N. Psychiatric co-morbidities in patients with chronic peripheral neuropathic pain: A multicentre cohort study. *Eur J Pain*. 2013;17(10):1547–1557.

2. Gerrits MMJG, et al. Impact of pain on the course of depressive and anxiety disorders. *Pain*. 2012;153(2):429–436.

3. Asmundson GJG, Katz J. Understanding the co-occurrence of anxiety disorders and chronic pain: state-of-the-art. *Depress Anxiety*. 2009;26(10):888–901.

4. Bair MJ, et al. Impact of Pain on Depression Treatment Response in Primary Care: *Psychosom Med*. 2004;66(1):17–22.

5. Hestehave S, et al. *Predicting hypersensitivity and comorbid depressive-like behavior in late stages of joint disease using early weight bearing deficit*. bioRxiv; 2023. doi: https://doi.org/10.1101/2023.11.29.569246 . *In Press* (Pain Reports).

6. Maiarù M, et al. The stress regulator FKBP51: a novel and promising druggable target for the treatment of persistent pain states across sexes. *Pain*. 2018;159(7):1224–1234.

7. Maiarù M, et al. The stress regulator FKBP51 drives chronic pain by modulating spinal glucocorticoid signaling. *Sci Transl Med*. 2016;8(325):325ra19.

8. Wanstrath BJ, et al. Duration of Reduction in Enduring Stress-Induced Hyperalgesia Via FKBP51 Inhibition Depends on Timing of Administration Relative to Traumatic Stress Exposure. *J Pain*. 2022;23(7):1256–1267.

9. Bortsov AV, et al. Polymorphisms in the glucocorticoid receptor co-chaperone FKBP5 predict persistent musculoskeletal pain after traumatic stress exposure. *Pain*. 2013;154(8):1419–1426.

10. Linnstaedt SD, et al. A Functional riboSNitch in the 3' Untranslated Region of *FKBP5* Alters MicroRNA-320a Binding Efficiency and Mediates Vulnerability to Chronic Post-Traumatic Pain. *J Neurosci*. 2018;38(39):8407–8420.

11. Lobo JJ, et al. Hippocampal volume, FKBP5 genetic risk alleles, and childhood trauma interact to increase vulnerability to chronic multisite musculoskeletal pain. *Sci Rep*. 2022;12(1):6511.

12. Zannas AS, et al. Gene–Stress–Epigenetic Regulation of FKBP5: Clinical and Translational Implications. *Neuropsychopharmacology*. 2016;41(1):261–274.

13. Hartmann J, et al. Pharmacological Inhibition of the Psychiatric Risk Factor FKBP51 Has Anxiolytic Properties. *J Neurosci Off J Soc Neurosci*. 2015;35(24):9007–9016.

14. Hartmann J, et al. The involvement of FK506-binding protein 51 (FKBP5) in the behavioral and neuroendocrine effects of chronic social defeat stress. *Neuropharmacology*. 2012;62(1):332–339.

15. Albu S, et al. Deficiency of FK506-binding protein (FKBP) 51 alters sleep architecture and recovery sleep responses to stress in mice. *J Sleep Res*. 2014;23(2):176–185.

16. O'Leary JC, et al. A new anti-depressive strategy for the elderly: ablation of FKBP5/FKBP51. *PloS One*. 2011;6(9):e24840.

17. Balsevich G, et al. Stress-responsive FKBP51 regulates AKT2-AS160 signaling and metabolic function. *Nat Commun*. 2017;8(1). https://doi.org/10.1038/s41467-017-01783-y.

18. Sabbagh JJ, et al. Age-Associated Epigenetic Upregulation of the FKBP5 Gene Selectively Impairs Stress Resiliency. *PLoS ONE*. 2014;9(9):e107241.

19. Touma C, et al. FK506 binding protein 5 shapes stress responsiveness: modulation of neuroendocrine reactivity and coping behavior. *Biol Psychiatry*. 2011;70(10):928–936.

20. Stechschulte LA, et al. FKBP51 Null Mice Are Resistant to Diet-Induced Obesity and the PPARγ Agonist Rosiglitazone. *Endocrinology*. 2016;157(10):3888–3900.

21. Gaali S, et al. Selective inhibitors of the FK506-binding protein 51 by induced fit. *Nat Chem Biol*. 2015;11(1):33–37.

22. Ardi Z, et al. Behavioral profiling as a translational approach in an animal model of posttraumatic stress disorder. *Neurobiol Dis*. 2016;88:139–147.

23. Sarkar I, et al. Individual behavioral profiling as a translational approach to assess treatment efficacy in an animal model of post-traumatic stress disorder. *Front Neurosci*. 2022;16:1071482.

24. Wedel S, et al. SAFit2 ameliorates paclitaxel-induced neuropathic pain by reducing spinal gliosis and elevating pro-resolving lipid mediators. *J Neuroinflammation*. 2023;20(1):149.

25. Häusl AS, et al. Mediobasal hypothalamic FKBP51 acts as a molecular switch linking autophagy to whole-body metabolism. *Sci Adv*. 2022;8(10):eabi4797.

26. Engelhardt C, et al. FKBP51 in the Oval Bed Nucleus of the Stria Terminalis Regulates Anxiety-Like Behavior. *eNeuro*. 2021;8(6):ENEURO.0425-21.2021.

27. Han Q, et al. SHANK3 Deficiency Impairs Heat Hyperalgesia and TRPV1 Signaling in Primary Sensory Neurons. *Neuron*. 2016;92(6):1279–1293.

28. Schaffler MD, Middleton LJ, Abdus-Saboor I. Mechanisms of Tactile Sensory Phenotypes in Autism: Current Understanding and Future Directions for Research. *Curr Psychiatry Rep*. 2019;21(12). https://doi.org/10.1007/s11920-019-1122-0.

29. Gu P, et al. Histone deacetylase 5 (HDAC5) regulates neuropathic pain through SRY-related HMG-box 10 (SOX10)-dependent mechanism in mice. *Pain*. 2018;159(3):526–539.

30. Mikaeili H, et al. Molecular basis of *FAAH-OUT*-associated human pain insensitivity. *Brain*. 2023;146(9):3851–3865.

31. Habib AM, Cox JJ, Okorokov AL. Out of the dark: the emerging roles of lncRNAs in pain. *Trends Genet*. 2024;40(8):694–705.

32. De Felice M, et al. Effects of Src-kinase inhibition in cancer-induced bone pain. *Mol Pain*. 2016;12:174480691664372.

33. Singleton S, Hales TG. Morphine-induced mechanical hypersensitivity in mice requires δ receptors, β-arrestin2, and c-Src activity. *J Physiol*. 2023;601(8):1483–1500.

34. Fang Y, et al. Astrocytic phosphatase and tensin homolog deleted on chromosome 10 regulates neuropathic pain by facilitating 3-hydroxy-3-methylglutaryl-CoA reductase–dependent cholesterol biosynthesis. *Pain*. 2022;163(12):e1192–e1206.

35. Fotio Y, et al. NAAA-regulated lipid signaling governs the transition from acute to chronic pain. *Sci Adv*. 2021;7(43):eabi8834.

36. Ogbonna AC, Clark AK, Malcangio M. Development of monosodium acetate-induced osteoarthritis and inflammatory pain in ageing mice. *Age Dordr Neth*. 2015;37(3):9792.

37. Ogbonna AC, et al. Pain-like behaviour and spinal changes in the monosodium iodoacetate model of osteoarthritis in C57Bl/6 mice: Pain and spinal changes in mouse MIA model of OA. *Eur J Pain*. 2013;17(4):514–526.

38. Pitcher T, Sousa-Valente J, Malcangio M. The Monoiodoacetate Model of Osteoarthritis Pain in the Mouse. *J Vis Exp*. [published online ahead of print: May 16, 2016];(111). https://doi.org/10.3791/53746.

39. Thakur M, et al. Characterisation of a Peripheral Neuropathic Component of the Rat Monoiodoacetate Model of Osteoarthritis. *PLoS ONE*. 2012;7(3):e33730.

40. De Sousa Valente J. The Pharmacology of Pain Associated With the Monoiodoacetate Model of Osteoarthritis. *Front Pharmacol*. 2019;10:974.

41. Harvey VL, Dickenson AH. Behavioural and electrophysiological characterisation of experimentally induced osteoarthritis and neuropathy in C57Bl/6 mice. *Mol Pain*. 2009;5:18.

42. Kobayashi K, et al. Sodium iodoacetate-induced experimental osteoarthritis and associated pain model in rats. *J Vet Med Sci*. 2003;65(11):1195–1199.

43. Ackerman IN, et al. The projected burden of osteoarthritis and rheumatoid arthritis in Australia: A population-level analysis. *Arthritis Care Res*. [published online ahead of print: September 12, 2017]. https://doi.org/10.1002/acr.23414.

44. Park J, Mendy A, Vieira ER. Various Types of Arthritis in the United States: Prevalence and Age-Related Trends From 1999 to 2014. *Am J Public Health*. 2017;e1–e3.

45. Axford J, et al. Prevalence of anxiety and depression in osteoarthritis: use of the Hospital Anxiety and Depression Scale as a screening tool. *Clin Rheumatol*. 2010;29(11):1277–1283.

46. Sharma A, et al. Anxiety and depression in patients with osteoarthritis: impact and management challenges. *Open Access Rheumatol Res Rev*. 2016;Volume 8:103–113.

47. Sellmeijer J, et al. Hyperactivity of Anterior Cingulate Cortex Areas 24a/24b Drives Chronic Pain-Induced Anxiodepressive-like Consequences. *J Neurosci Off J Soc Neurosci*. 2018;38(12):3102–3115.

48. Hestehave S, et al. The influence of rat strain on the development of neuropathic pain and comorbid anxio-depressive behaviour after nerve injury. *Sci Rep*. 2020;10(1):20981.

49. Dimitrov EL, et al. Anxiety- and depression-like behavior and impaired neurogenesis evoked by peripheral neuropathy persist following resolution of prolonged tactile hypersensitivity. *J Neurosci Off J Soc Neurosci*. 2014;34(37):12304–12312.

50. Urban R, et al. Behavioral indices of ongoing pain are largely unchanged in male mice with tissue or nerve injury-induced mechanical hypersensitivity. *Pain*. 2011;152(5):990–1000.

51. Gebru NT, et al. *Fkbp5* gene deletion: Circadian rhythm profile and brain proteomics in aged mice. *Aging Cell*. 2024;e14314.

52. Codagnone MG, et al. Inhibition of FKBP51 induces stress resilience and alters hippocampal neurogenesis. *Mol Psychiatry*. 2022;27(12):4928–4938.

53. Hähle A, et al. The Many Faces of FKBP51. *Biomolecules*. 2019;9(1):35.

54. Ma X, Peterson R, Turnbull J. Adenylyl Cyclase type 3, a marker of primary cilia, is reduced in primary cell culture and in lumbar spinal cord in situ in G93A SOD1 mice. *BMC Neurosci*. 2011;12(1). https://doi.org/10.1186/1471-2202-12-71.

55. Tucker K, et al. The Primary Cilium and its Hedgehog Signaling in NociceptorsContribute to Inflammatory and Neuropathic Pain [preprint]. 2024. https://doi.org/10.21203/rs.3.rs-3812442/v1.

56. Fagan RR, et al. Selective targeting of mu opioid receptors to primary cilia. *Cell Rep*. 2024;43(5):114164.

57. Walwyn WM, et al. Sustained Suppression of Hyperalgesia during Latent Sensitization by μ-, δ-, and κ-opioid receptors and α_{2A} Adrenergic Receptors: Role of Constitutive Activity. *J Neurosci*. 2016;36(1):204–221.

58. Massing U, Cicko S, Ziroli V. Dual asymmetric centrifugation (DAC)--a new technique for liposome preparation. *J Control Release Off J Control Release Soc*. 2008;125(1):16–24.

59. Dixon WJ. Efficient Analysis of Experimental Observations. *Annu Rev Pharmacol Toxicol*. 1980;20(1):441–462.

60. Maiarù M, et al. Substance P-Botulinum Mediates Long-term Silencing of Pain Pathways that can be Re-instated with a Second Injection of the Construct in Mice. *J Pain*. 2024;25(6):104466.

61. Learoyd AE, Sen D, Fitzgerald M. The pain trajectory of juvenile idiopathic arthritis (JIA): translating from adolescent patient report to behavioural sensitivity in a juvenile animal model. *Pediatr Rheumatol*. 2019;17(1):60.

62. Ängeby Möller K, et al. Pain behaviour assessments by gait and weight bearing in surgically induced osteoarthritis and inflammatory arthritis. *Physiol Behav*. 2020;225:113079.

63. Berrio JP, Hestehave S, Kalliokoski O. Reliability of sucrose preference testing following short or no food and water deprivation—a Systematic Review and Meta-Analysis of rat models of chronic unpredictable stress. *Transl Psychiatry*. 2024;14(1):39.

64. Brown LA, et al. COMPASS: Continuous Open Mouse Phenotyping of Activity and Sleep Status. *Wellcome Open Res*. 2016;1:2.

65. Brown L, et al. Telling the Time with a Broken Clock: Quantifying Circadian Disruption in Animal Models. *Biology*. 2019;8(1):18.

66. Conesa A, et al. A survey of best practices for RNA-seq data analysis. *Genome Biol*. 2016;17:13.

67. Mills C, et al. Estimating Efficacy and Drug ED50's Using von Frey Thresholds: Impact of Weber's Law and Log Transformation. *J Pain*. 2012;13(6):519–523.

Figures

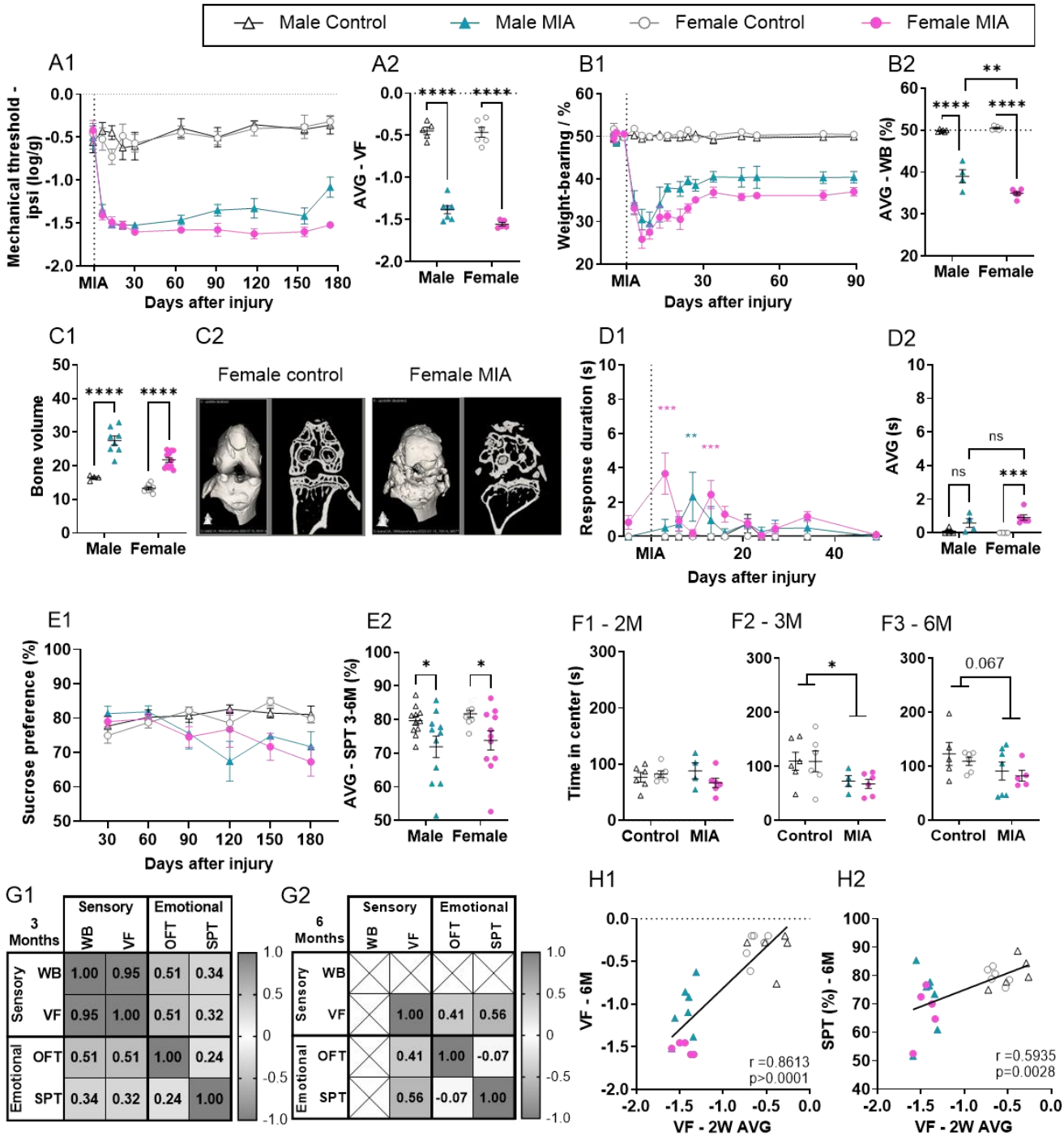

Figure 1: MIA induces immediate and persistent sensory and functional changes, but delayed anxio-depressive comorbidities. (A1,2) Mechanical hypersensitivity was assessed using Von Frey (VF) filaments and followed for 6 months (N=5-7). **(B1,2)** Functional deficit was assessed using static weight bearing (WB) distribution and followed for 3 months after injury (N=4-6). **(C1,2)** Joint deformation was assessed by exploring the bone volume around the joint, as assessed using microCT at 6 months after injury (N=4-11). Pictures of female control and MIA examples are presented in C2. **(D1,2)** The duration of the affective response following the application of a 0.04g vF filament was recorded in seconds and followed for 49 days after injury (N=4-6). **(E1,2)** Depressive-like behavior (anhedonia) was assessed using the Sucrose Preference Test (two bottle test, water vs 1% sucrose), and was followed monthly for 6

months after injury. Weighted average (AVG) was calculated from 3-6months. (N=4-12). **(F1,2,3)** Anxiety-like behavior was assessed using the Open Field Test, and was measured at 2 (F1), 3 (F2) and 6 (F3) months after injury, assessing the time spent in the center of the arena (N=4-7). **(G1,2)** Summary of correlations between outcomes recorded on the same animal at the same time point at 3 (G1) and 6 (G2) months (N=22-23 across groups). **(H1,2)** Correlations between early (2week weighted average) of mechanical sensitivity and the later stage of hypersensitive - (H1) and depressive-like (H2) behavior at 6 months. For fig A2, B2, D2: Weighted average (AVG) was calculated across the full study period. For all graphs; data shows mean ± S.E.M. NS= Not significant, *P<0.05, **P<0.01, ***P<0.001, ****P<0.0001, as determined using appropriate post-test, or for fig F1,2,3 determined by 2way ANOVA. See full statistical analysis in Supplementary Table S1.

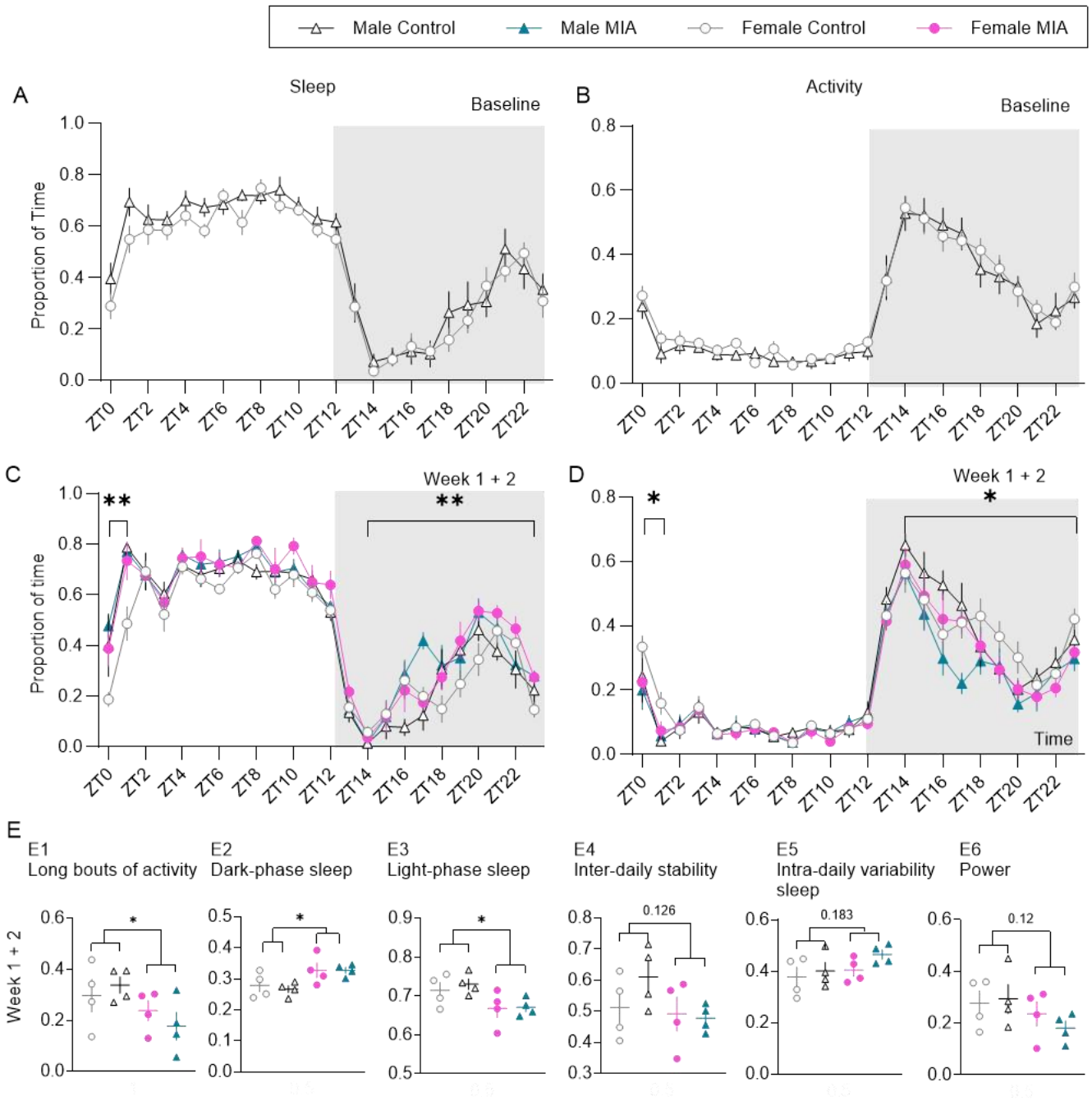

Figure 2: MIA-induced joint pain is accompanied by disruption to circadian patterns. (A-D) 24h activity/sleep plots using 1h bins. **(A, B)** Average of 24h plots across the 6 days before MIA injection. N=8/8. There were no differences in sleep (A) and activity (B) patterns in naive, 8-week-old male and female mice. **(C, D)** Average of 24h plots across the first 2 weeks after MIA injection. N=4/4/4/4. **(E) (E1)** proportion of time spent in long bouts (>10min) activity during the dark period, **(E2)** proportion of time spent in sleep during the dark phase, **(E3)** proportion of time spent in sleep during the light phase, **(E4)** interdaily stability, **(E5)**, intra-daily variability sleep and **(E6)** power of the 24-hour activity cycle calculated across 2 weeks. The power of a periodogram provides a measure of the strength and regularity of the underlying rhythm, with higher values indicating robust rhythms. In circadian disruption—where rhythms are typically less robust—the power is expected to be reduced, which may indicate the absence of a significant circadian rhythm. N=4/4/4/4. ZT0=7am, ZT12=7pm. Data shows mean ± S.E.M. *P<0.05; ** P<0.01, injury effect. See full statistical analysis in Supplementary Table S1.

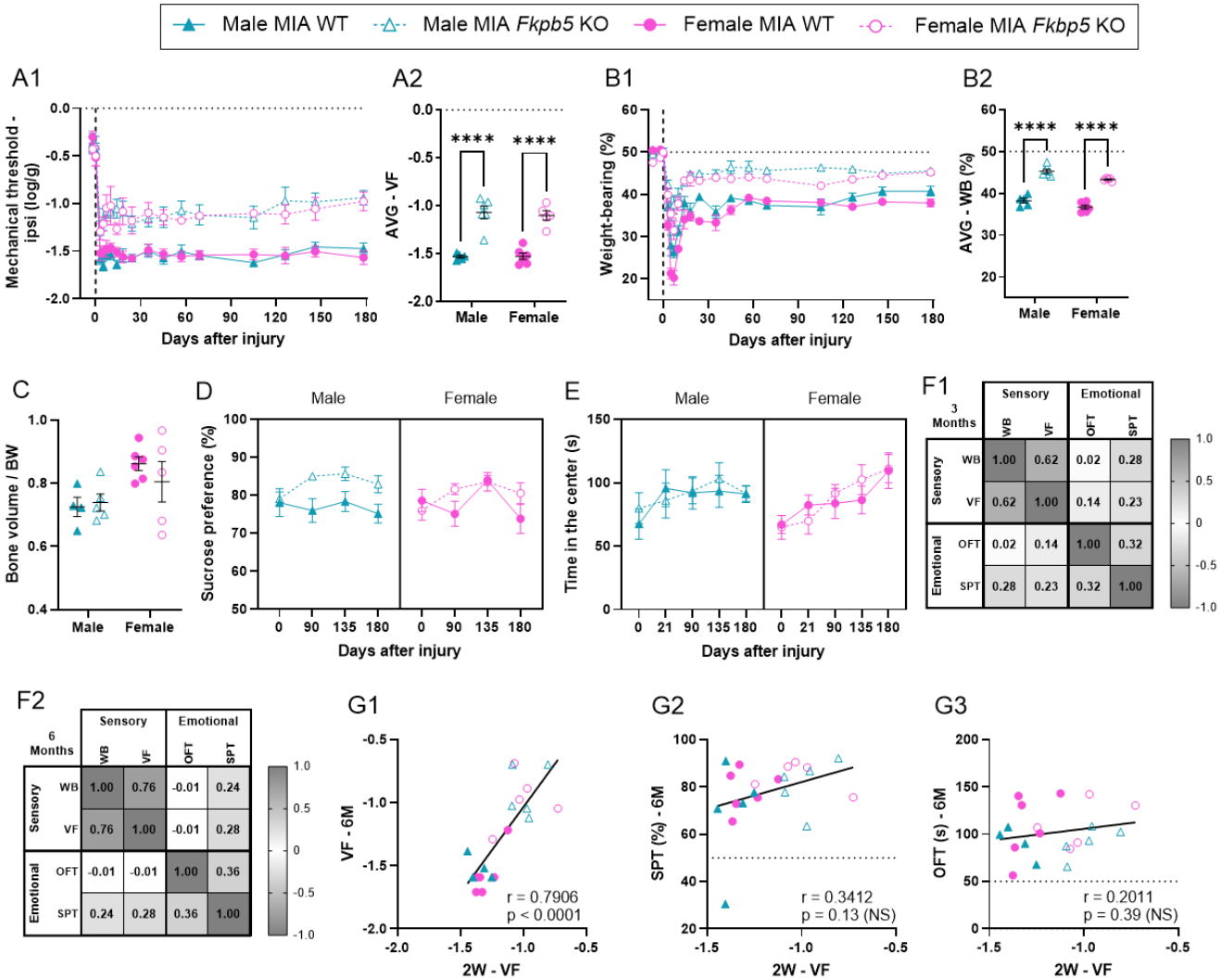

Figure 3: *Fkbp5* global knockdown improves sensory, functional and depressive-like behavior induced by MIA. Male and female *Fkbp5* KO and WT littermates were all exposed to MIA and followed for 6 months after injection. **(A1,2)** Mechanical hypersensitivity was assessed using von Frey filaments (N=5-6). **(B1,2)** Functional deficits were assessed using static weight bearing distribution (N=5-6). **(C)** Joint deformation was assessed by exploring the bone volume around the joint using microCT at 6 months after injury and normalised to body weight to account for differences in body-size (N=4-6). **(D)** Depressive-like behavior (anhedonia) was assessed using the Sucrose Preference Test (two-bottle test, water vs 1% sucrose) (N=5-9). **(E)** Anxiety-like behavior was assessed using the Open Field Test, measuring the time in the center of the arena (N=5-6). **(F1,2)** Summary of correlations between outcomes recorded on the same animal at the same time point at 3 (F1) and 6 (F2) months (N=22 across groups). **(G1,2,3)** Correlations between early (2week weighted average) of mechanical sensitivity and the later level/development of pain- (G1), depressive- (G2) and anxiety-like (G3) behavior at 6 months. For fig A2, B2: Weighted average (AVG) was calculated across the full study period. For all graphs; data shows mean ± S.E.M. *P<0.05, **P<0.01, ***P<0.001, ****P<0.0001, as determined using appropriate post-test. See full statistical analysis in Supplementary Table S1.

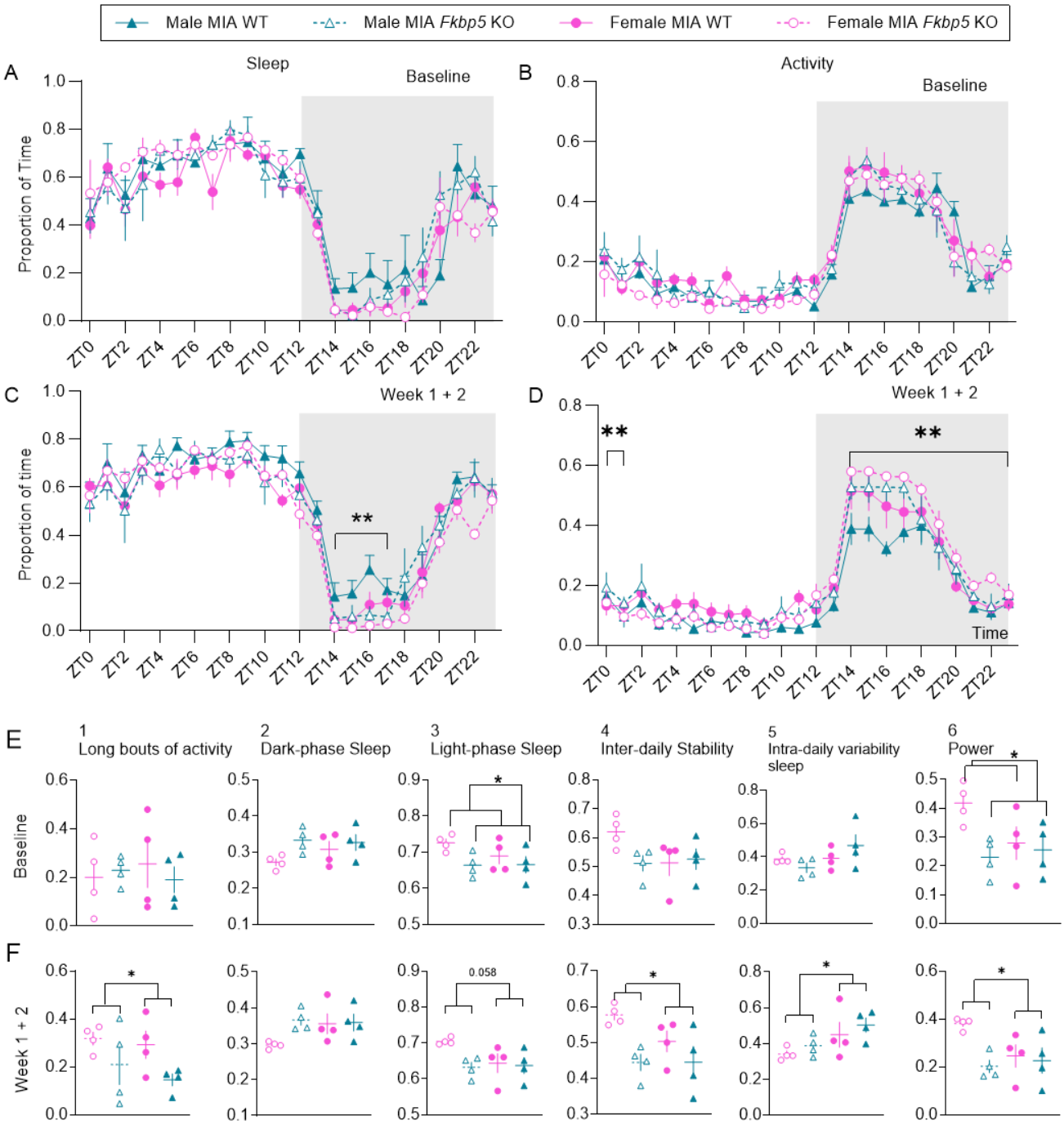

Figure 4: *Fkbp5* global knockdown improves some of the MIA-induced changes to circadian patterns. (A-D) 24h activity/sleep plots using 1h bins. **(A, B)** Average of 24h plots across the 6 days before MIA injection. N=8/8. There were no differences in sleep (A) and activity (B) patterns in naive, 8-week-old male and female, WT and KO mice. **(C, D)** Average of 24h plots across the first 2 weeks after MIA injection. N=4/4/4/4. *Fkbp5* knock-down improved some of the MIA induced changes to sleep and activity patterns. **(E,F) (1)** Proportion of time spent in long bouts (>10min) activity during the dark period, **(2)** proportion of time spent in sleep during the dark phase, **(3)** proportion of time spent in sleep during the light phase, **(4)** interdaily stability, **(5)**, intra-daily variability sleep and **(6)** A power of the 24-hour activity cycle . (E) Average across 6 days before MIA. (F) Average across first 2 weeks after MIA. N=4/4/4/4. Data shows mean ± S.E.M. *P<0.05; ** P<0.01, genotype effect. (E6) sex effect plotted. See full statistical analysis in Supplementary Table S1.

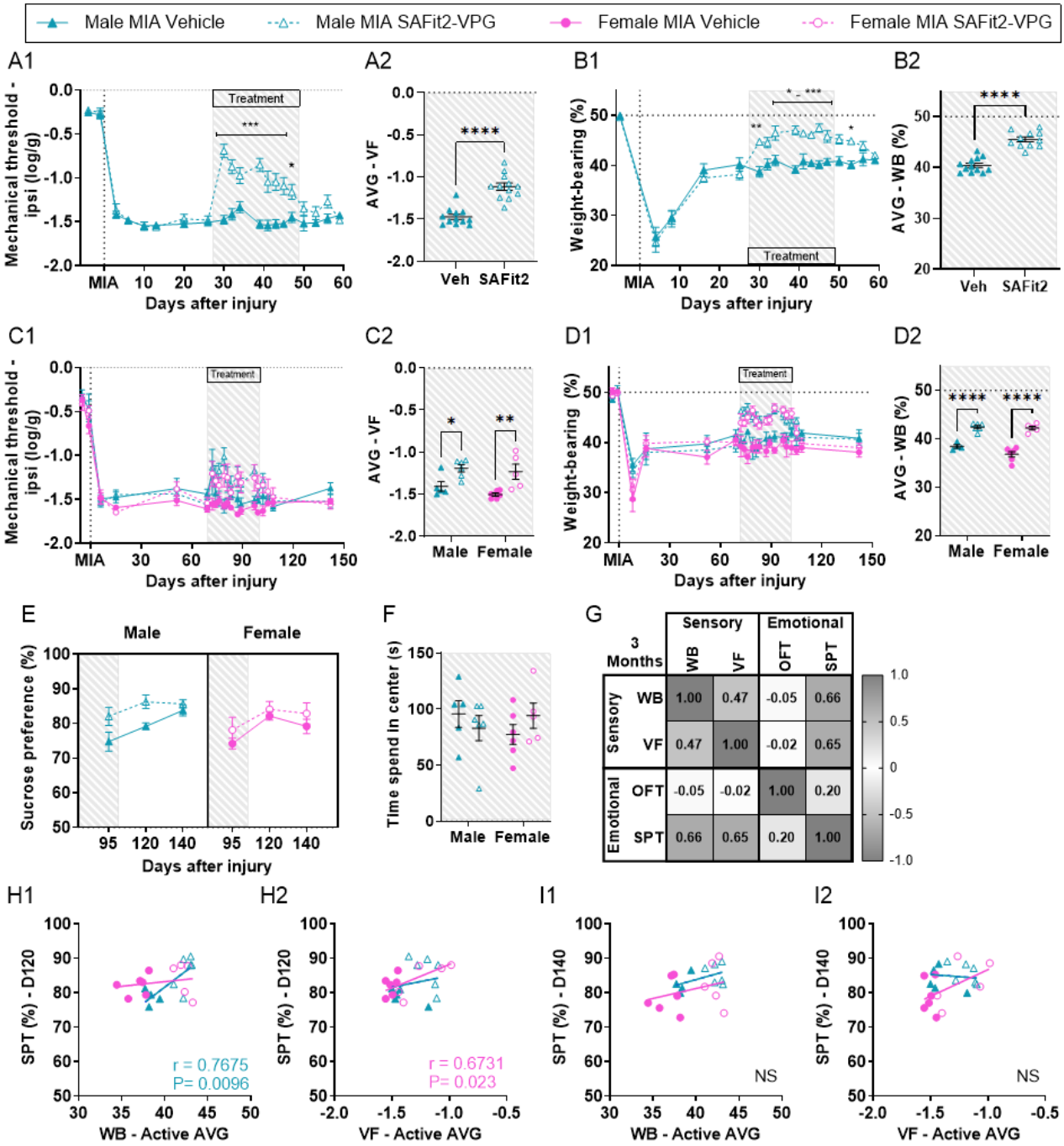

Figure 5. Pharmacological inhibition of FKBP51 after MIA induction improves sensory and functional deficits and delays the onset of depressive-like behaviors. All mice were subjected to MIA-injury, and SAFit2-VPG was administered at different time points after injury, hatched grey area indicates when compound was active. (**A1,2**) SAFit2-VPG produced significant improvements on mechanical hypersensitivity when administered from 4-6 weeks after injury in male mice. (N=12). (**B1,2**) SAFit2-VPG produced significant improvements on weight bearing asymmetry when administered from 4-6 weeks after injury in male mice. (N=11-12). (**C1,2**) SAFit2-VPG produced significant improvements on mechanical hypersensitivity when administered from 10-14 weeks after injury. (N=5-6). (**D1,2**) SAFit2-VPG produced significant improvements on weight bearing asymmetry when administered from 10-14 weeks after injury. (N=4-6). (**E**) Depressive-like behavior (sucrose preference test) was improved by administration of SAFit2-VPG at 10-14weeks. First measure was performed ~D95 (in week 14), while the compound

was still active, and post-active measured were performed at Day 120 (3 weeks after the active phase) and Day 140 (6 weeks after active phase) (N=5-6). (**F**) Anxiety-like behavior at ~3 months (14 weeks after injury) was unaffected by administration of SAFit2-VPG from 10-14 weeks (N=5-6). (**G**) Summary of correlations between outcomes recorded on the same animal at the same time point at 3 months after injury (14 weeks), when SAFit2-VPG was administered from 10-14 weeks after injury (N=21 across groups). (**H1,2**) Correlations between the weighted average weight bearing asymmetry (WB) or mechanical hypersensitivity (VF) from the active phase of administration (10-14weeks) and the level of depressive-like behavior 3 weeks after the active phase. (**I1,2**) Correlations between the weighted average weight bearing asymmetry (WB) or mechanical hypersensitivity (VF) from the active phase of administration (10-14weeks) and the level of depressive-like behavior 6 weeks after the active phase were not significant. For fig A2, B2, C2, D2: Weighted average (AVG) was calculated for the hatched grey study period, where the compound was active. For all graphs; data shows mean ± S.E.M. *P<0.05, **P<0.01, ***P<0.001, ****P<0.0001, as determined using appropriate post-test. See full statistical analysis in Supplementary Table S1.

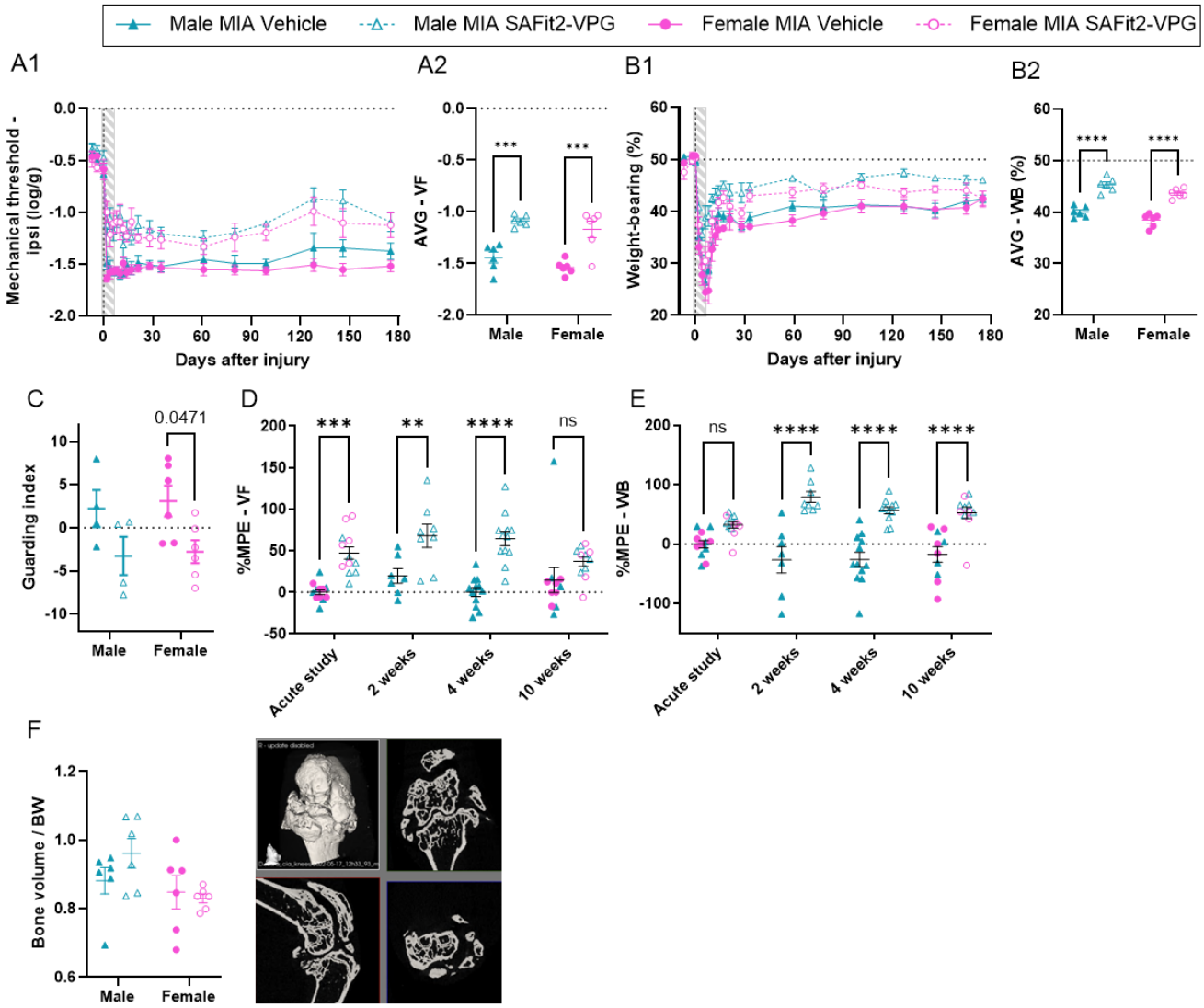

Figure 6. Acute pharmacological inhibition of FKBP51 initiated before MIA induction prevents the full development of sensory and functional deficits. All mice were subjected to MIA-injury and SAFit2-VPG was administered from 3 days before and lasting for approximately 14 days (*i.e.* 11 days after injury), hatched grey area suggests when the compound was active. (**A1,2**) Early treatment with SAFit2-VPG produced a significant and persistently lower level of mechanical hypersensitivity from MIA injury, which lasted much beyond the active phase of the compound (N=6). (**B1,2**) Early treatment with SAFit2-VPG produced a significant and persistently lower level of weight bearing asymmetry from MIA injury, which lasted much beyond when the compound was active (N=6). (**C**) Catwalk gait analysis showed a significantly lower guarding index at 6 weeks after injury, following early SAFit2-VPG treatment around onset of injury (N=4-6). (**D**) %MPE for the mechanical sensitivity was calculated for the first measure after the first injection of SAFit2-VPG in the different studies (D3 for post-MIA treatment studies, and day 2 for pre-MIA/acute treatment), for comparison across studies (N=7-12). (**E**) %MPE for the weight bearing asymmetry was calculated for the first measure after the first injection of SAFit2-VPG in the different studies (D3 for post-MIA treatment studies, and day 2 for pre-MIA/acute treatment), for comparison across studies (N=7-12). (**F**) Joint deformation at 6 months after injury was unaltered by early treatment with SAFit2-VPG (N=6). For fig A2, B2: Weighted average (AVG) was calculated for the full study period. For all graphs; data shows mean ± S.E.M. *P<0.05, **P<0.01, ***P<0.001, ****P<0.0001, as determined using appropriate post-test. See full statistical analysis in Supplementary Table S1.

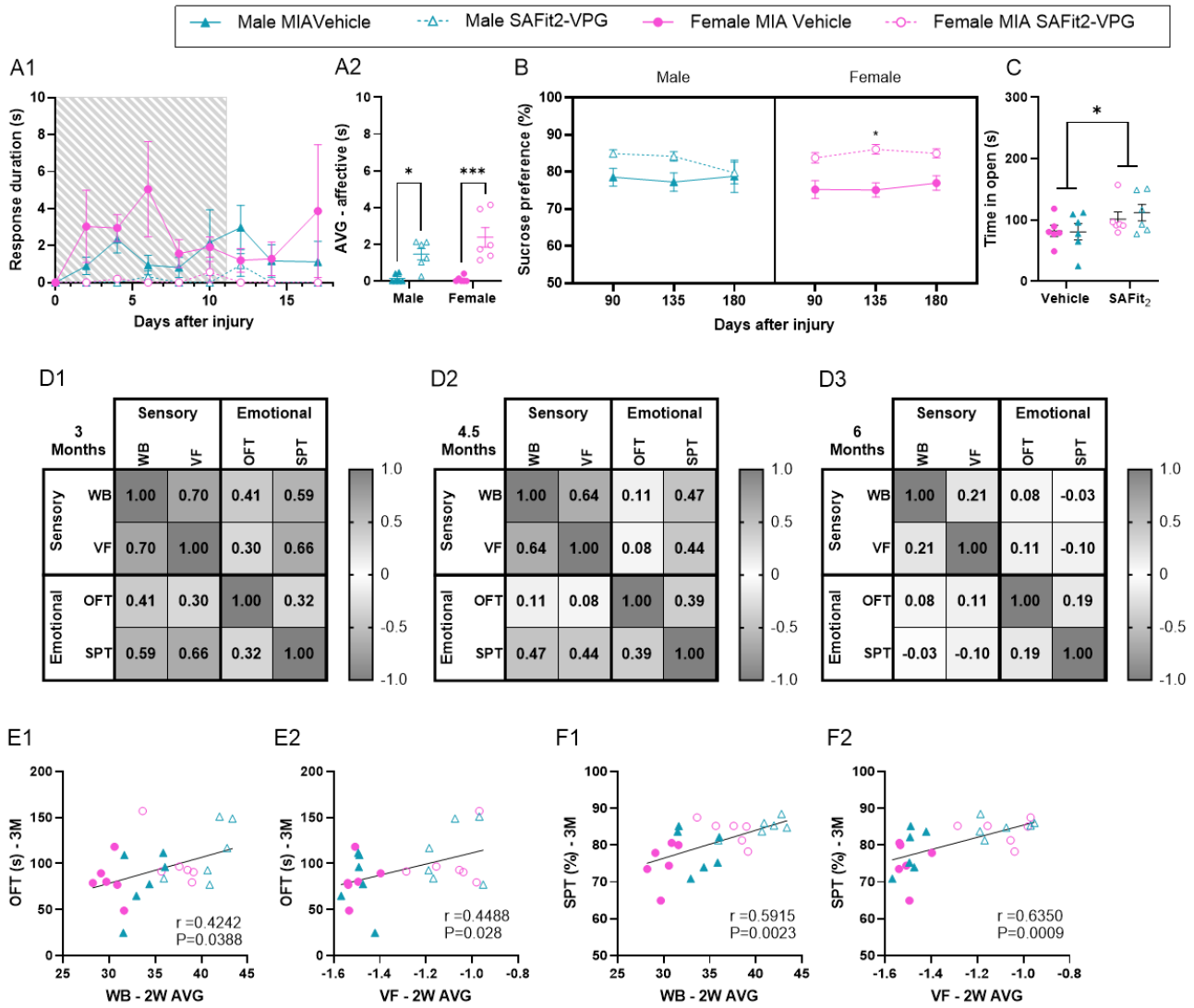

Figure 7. Acute pharmacological inhibition of FKBP51 initiated before MIA induction delays the onset of anxiety- and depressive-like behaviors. All mice were subjected to MIA-injury and SAFit2-VPG was administered from 3 days before and lasting for approximately 11 days after injury, hatched grey area suggests when the compound was active. (**A1,2**) Early treatment with SAFit2-VPG produced a significant lower level of affective responding to mechanical stimulation with a low intensity filament (0.04g) following MIA injury. Weighted average (AVG) was calculated for the full study period. (N=6). (**B**) Early treatment with SAFit2-VPG completely prevented (females) or delayed (males) the development of depressive-like behaviors at 3-6 months after injury (N=6). (**C**) Early treatment with SAFit2-VPG significantly decreased the level of anxiety-like behavior at 3 months after injury (N=6). (**D1,2,3**) Summary of correlations between outcomes recorded on the same animal at the same time point at 3 (**D1**), 4.5 (**D2**) and 6 (**D3**) months after injury, when SAFit2-VPG was administered around the onset of injury (N=24 across groups). (**E1,2**) Correlations between the weighted average weight bearing asymmetry (WB) or mechanical hypersensitivity (VF) from the first two weeks after injury, when the compound was active, and the level of anxiety-like behavior at 3 months. (**F1,2**) Correlations between the weighted average weight bearing asymmetry (WB) or mechanical hypersensitivity (VF) from the first two weeks after injury, when the compound was active and the level of depressive-like behavior at 3 months. For all graphs; Error bars suggest Mean ± S.E.M. *P<0.05, **P<0.01, ***P<0.001, as determined using appropriate post-test, or for fig C by 2way ANOVA. See full statistical analysis in Supplementary Table S1.

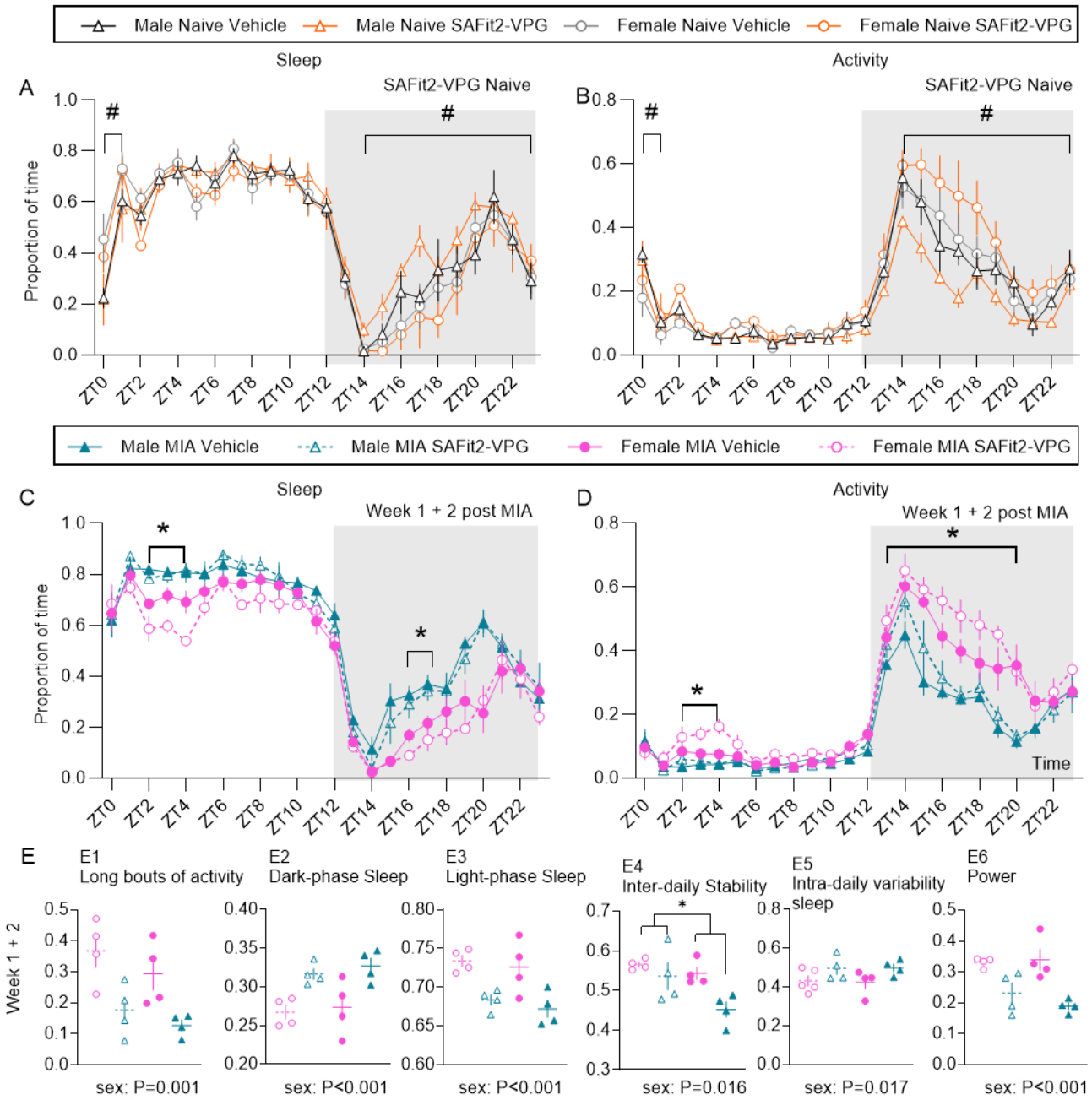

Figure 8: Pharmacological inhibition of FKBP51 reverses a number of MIA-induced changes to circadian patterns. (A-D) 24h activity/sleep plots using 1h bins. **(A, B)** Average of 24h plots across the 6 days of SAFIt2-VPG exposure. N=8/8. SAFit2 alone induces changes to sleep (A) and activity (B) patterns in naive, 8-week-old male and female mice. **(C, D)** Average of 24h plots across the first 2 weeks after MIA injection. N=4/4/4/4. SAFit2 reversed some of the MIA induced changes to sleep and activity patterns. **(E)** Average across 14 days after MIA. **(E1)** Proportion of time spent in long bouts (>10min) activity during the dark period, **(E2)** proportion of time spent in sleep during the dark phase, **(E3)** proportion of time spent in sleep during the light phase, **(E4)** interdaily stability, **(E5)** intra-daily variability sleep and **(E6)** power of the 24-hour activity cycle calculated across 2 weeks. N=4/4/4/4. Data shows mean ± S.E.M. # P<0.05, sex effect within SAFit treated group; *P<0.05; treatment effect (3-way ANOVA). See full statistical analysis in Supplementary Table S1.

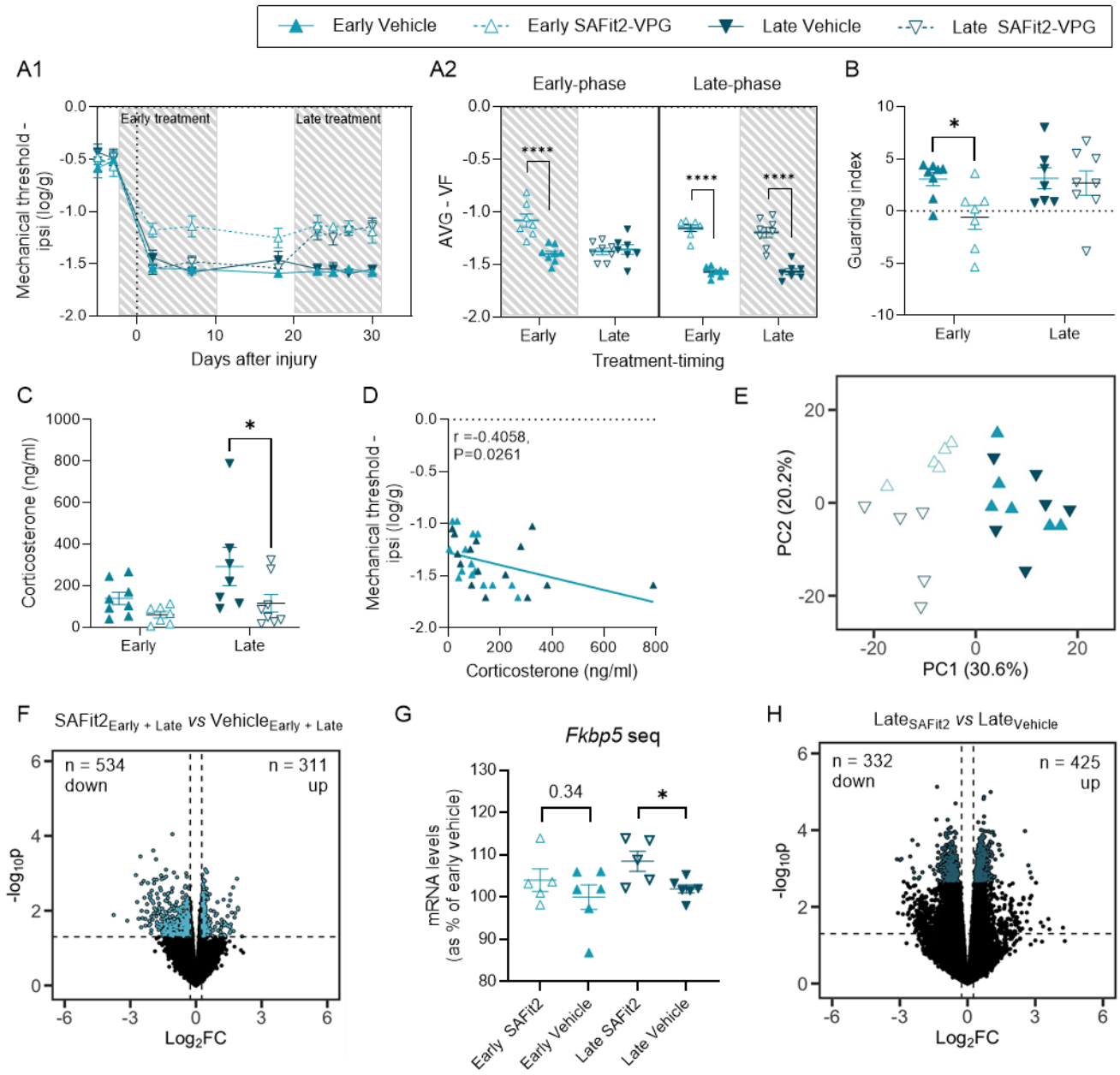

Figure 9. Pharmacological inhibition of FKBP51 initiated before or after MIA induction leads to different gene expression changes. All male mice were subjected to MIA-injury, and SAFit2-VPG was administered either "Early" from 3 days before and lasting for approximately 11 days after injury, or "Late" from D20-30, hatched grey area suggests when the compound was active. (**A1,2**) Early treatment with SAFit2-VPG produced long-term improvement of mechanical hypersensitivity, of similar degree as "late" treatment once given, as suggested by both the time course data (**A1**) and weighted average of measures recorded in the early vs late phase of the experiment (**A2**). (**B**) Catwalk gait analysis showed a significantly lower guarding index at D23 after injury for "Early" SAFit2-VPG treatment only. (**C**) Corticosterone measured at study-end (Day 31) was significantly lower for groups receiving SAFit2-VPG treatment across the two treatment timings, but also affected by treatment-timing (ANOVA: P=0.053), as the late treatment-groups generally had higher levels. (**D**) There was a significant correlation between the level of mechanical allodynia and corticosterone measured at the end of the experiment. (**E**) Principal Component Analysis (PCA) reveals sub-clusters within the second principal component of SAFit2-treated groups exposed at the early *vs* late time points which is not present in vehicle-treated groups (**F**) Volcano plots; x-axis: log2-transformed fold change in gene expression between SAFit2 and vehicle treated groups; y-axis represents the –log10(p-value)

for differential expression; coloured points are significantly up- or down-regulated with threshold abs(log2FC) >1.2; vertical dotted lines represent log2FC thresholds: left: log2FC=-1 (2 fold downregulation) and right: log2FC=1 (2 fold upregulation); horizontal dotted line represents the p-value threshold (**G**) expression levels of *Fkbp5* mRNA from sequencing counts, normalised to Early Vehicle (**H**) Volcano plots; x-axis: log2-transformed fold change in gene expression between $Late_{SAFit2}$ and $Late_{vehicle}$ treated groups; y-axis represents the –log10(p-value) for differential expression; coloured points are significantly up- or down-regulated with threshold abs(log2FC) >1.2; vertical dotted lines represent log2FC thresholds: left: log2FC=-1 (2 fold downregulation) and right: log2FC=1 (2 fold upregulation); horizontal dotted line represents the p-value threshold. For all graphs; (N=7-8), data shows Mean ± S.E.M. *P<0.05, ****P<0.0001, as determined using appropriate post-test. See full statistical analysis in Supplementary Table S1.

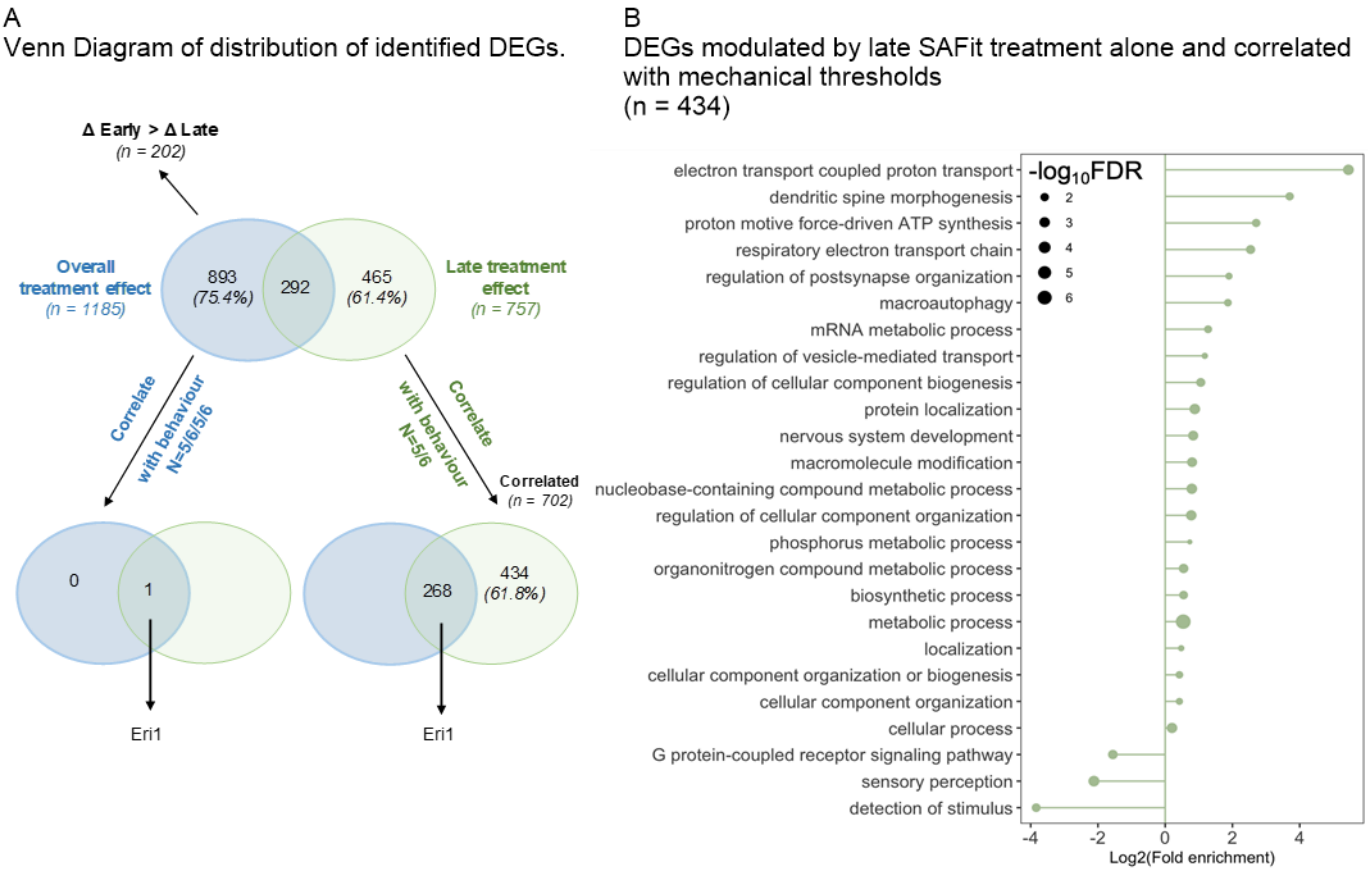

Figure 10: Late SAFit2-VPG treatment leads to changes in gene expression that correlate with mechanical hypersensitivity. (**A**) Venn Diagram of distribution of identified DEGs. (**B**) Lollipop plot of enriched GO terms after gene expression analysis. This figure displays the enriched Gene Ontology (GO) terms identified from the differentially expressed genes (DEGs) between $Late_{SAFit2}$ and $Late_{Vehicle}$ treated mice. The X-axis represents GO terms associated with biological processes while the Y-axis shows the fold change in enrichment. Significance (-log10 adjusted P-value) of each term is denoted by size.

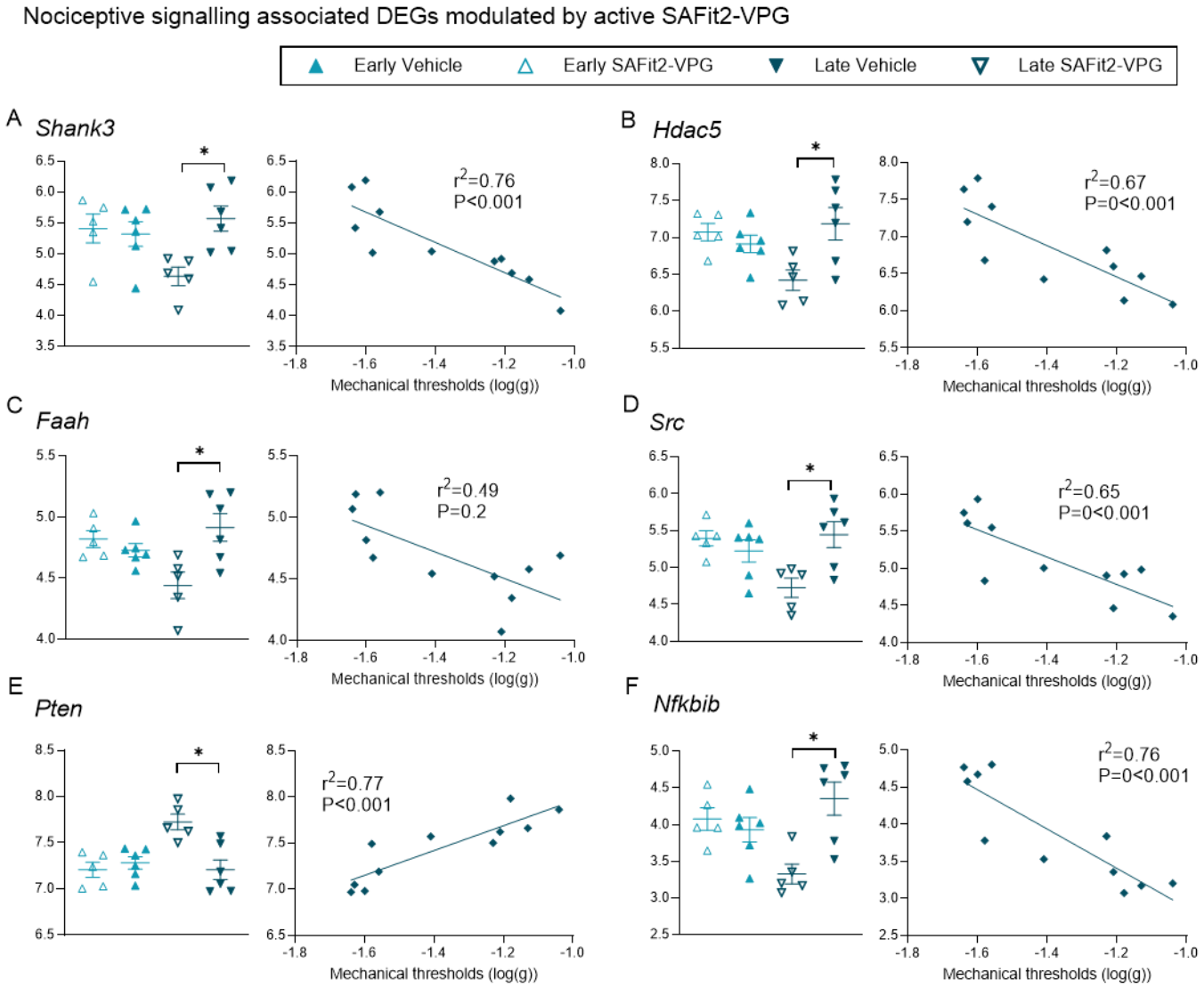

Figure 11: Late SAFit2-VPG treatment leads to changes in gene expression in nociceptive genes that correlate with mechanical hypersensitivity. DEGs by SAFit2-VPG late treatment associated with nociceptive signalling. *P<0.05, as per nested analysis; correlation graphs show the results of Pearson Correlation analysis. Y-axis: $\log_2$CPM. See full statistical analysis in Supplementary Table S1.

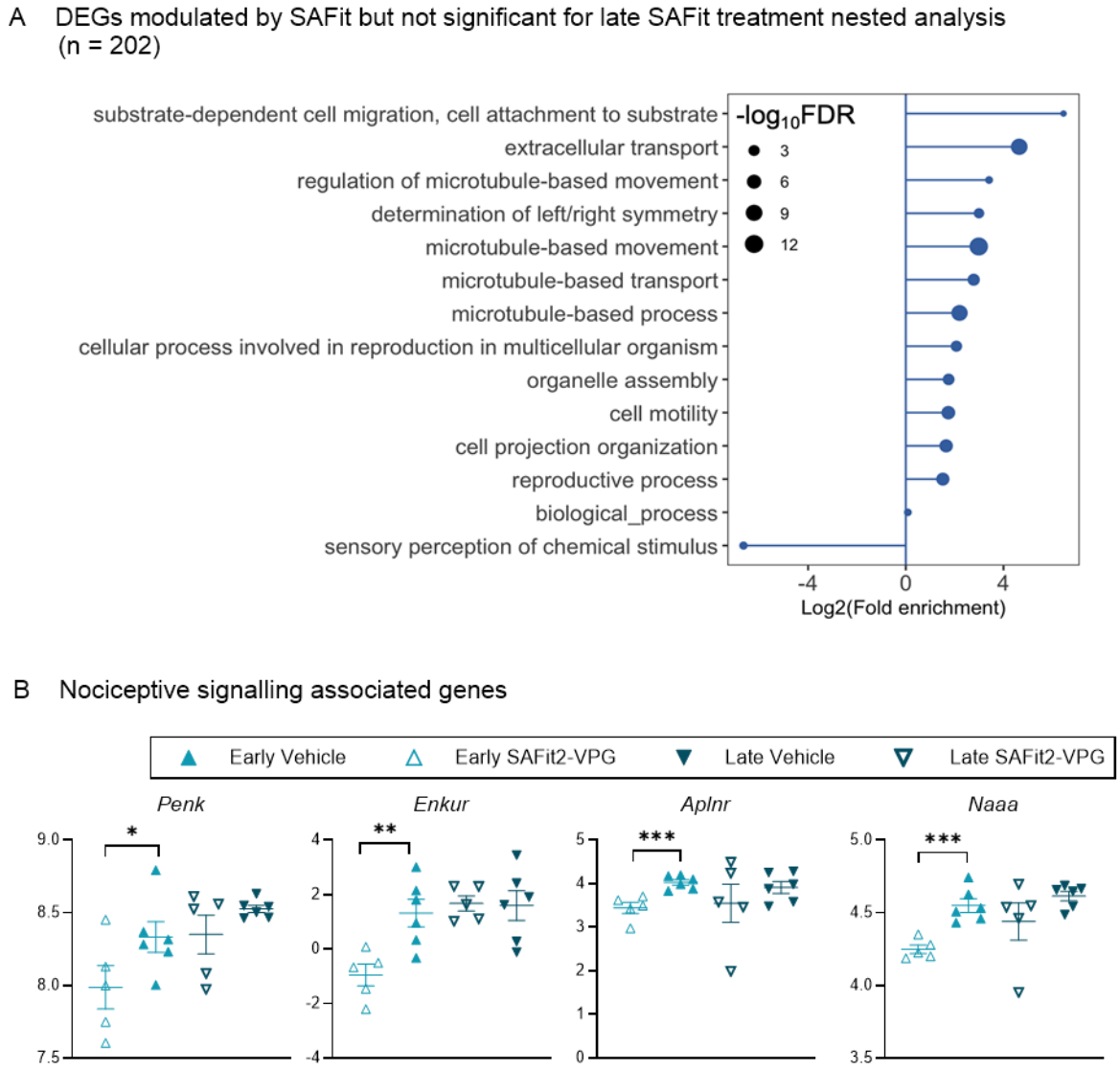

Figure 12: Early SAFit2-VPG treatment modulates the expression of genes related to cilia and nociceptive signalling. (**A**) Lollipop plot of enriched Gene Ontology (GO) terms after gene expression analysis. This figure displays the enriched GO terms identified by PANTHER from the differentially expressed genes (DEGs) between SAFit2 and vehicle treated mice, with an emphasis on genes with a greater change in expression between ($Early_{SAFit2}$ vs $Early_{Vehicle}$) than ($Late_{SAFit2}$ vs $Late_{Vehicle}$). The X-axis represents the GO terms related to biological processes while the Y-axis shows the fold change in enrichment. Significance (-log10 adjusted P-value) of each term is denoted by size. (**B**) Selected genes associated with nociceptive signalling. Y-axis: log_2CPM. *P<0.05; **P<0.01; ***P<0.001, t-test $Early_{SAFit2}$ vs $Early_{Vehicle}$.

Table 1. Percentage of mice "affected" by affective comorbidities associated with chronic joint pain

% Affected mice	Depressive-like behaviour				Anxiety-like behaviour	
Time (months)	3M	4M	5M	6M	3M	6M
MIA Females	54.5	0	80	100	45	80
MIA Males	25	75	25	42.9	27	43
Control Females	16.7	16.7	16.7	16.7	8.3	33.3
Control Males	20	0	25	20	9.1	20

Table 2. Percentage of mice "resilient" to affective behaviour associated with chronic joint pain (*Fkbp5* KO and WT).

% Resilient mice	Depressive-like behaviour				Anxiety-like behaviour			
Time (months)	0M	3M	4.5M	6M	0M	3M	4.5M	6M
WT Females	16.7	12.5	12.5	11.1	16.7	16.7	16.7	25
WT Males	20	14.3	14.3	12.5	20	20	20	16.7
KO Females	0	37.5	25	44.4	20	20	40	12.5
KO Males	0	50	50	55.6	33.3	16.7	16.7	28.6

Table 3. Percentage of mice "resilient" to affective behaviours associated with chronic joint pain following FKBP51 inhibition 2 months after injury. "Active" = while the compound was active, "Post" = 3 weeks after the end of the active period, "Late" = 6 weeks after end of active period.

% Resilient mice	Depressive-like behaviour			Anxiety-like behaviour	
Time	Active	Post	Late	Active	Post
Veh Females	16.7	16.7	33.3	16.7	16.7
Veh Males	20	0	20	20	0
SAFit2 Females	40	60	40	20	20
SAFit2 Males	50	83.3	33.3	0	16.7

Table 4. Percentage of mice "resilient" to affective behaviours associated with chronic joint pain following FKBP51 inhibition during disease onset.

% Resilient mice	Depressive-like behaviour			Anxiety-like behaviour		
Time (months)	3M	4.5M	6M	3M	4.5M	6M
Veh Females	0	16.7	16.7	16.7	33.3	16.7
Veh Males	16.7	16.7	0	0	50	16.7
SAFit2 Females	83.3	100	83.3	16.7	50	0
SAFit2 Males	66.7	33.3	16.7	50	33.3	16.7

Table 5: Study design.

Experiment purpose	**Groups**	**Tests**	**Figures**	**Total N** (note)
Characterization of MIA-induced changes (3-6 months)	MIA vs control (male vs female)	WB, VF, affective-VF, SPT, OFT,	Fig 1 + S1	22+23 (lost: 3)
		Sleep/activity, BV	Fig 2 + S2-4, Fig 1C	32
		Corticosterone	Fig S1	32
Effects of *Fkbp5* genetic manipulation on MIA-induced changes (6 months)	KO vs WT (male vs female) All MIA-injured	WB, VF, BV, SPT, OFT, EPM	Fig 3 + S5	22
		Sleep/activity, (SPT)	Fig 4 + S6-8	16
		Corticosterone	Fig S5	8
Effects of FKPB51 inhibition after MIA-injury (3 weeks, 2 months, 4-5months)	SAFit2-VPG vs VPG/vehicle, (Only males or male vs female) All MIA-injured	WB, VF, SPT, OFT, EPM	Fig 5 + S9	S9.A-B.: 15 (lost:1) 5A-B: 24 5C-I: 22 (lost: 2)
Effects of FKBP51 inhibition in naïve animals (4 weeks)	SAFit2-VPG vs VPG/vehicle, (male vs female) All naïve	OFT, VF, SPT 1%, SPT 0.5%	Fig S10	16
		Sleep / activity	Fig 8 + S13	16
Effects of FKPB51 inhibition at MIA-injury onset. (6months)	SAFit2-VPG vs VPG/vehicle, (male vs female) All MIA-injured	WB, VF, BV, affective-VF, SPT, OFT,	Fig 6-7 + S11-12	24
		Sleep / activity, catwalk	Fig 8 + S14-	20
RNA sequencing of early vs late treatment (30 days)	SAFit2-VPG vs VPG/vehicle, (male only) All MIA-injured	VF, catwalk, corticosterone, RNA sequencing.	Fig 9-11 + S15-18	30 (lost: 2)

Abbreviations: VF = von Frey. WB = weight bearing. OFT = Open Field Test. SPT = Sucrose Preference Test. EPM = Elevated Plus Maze. BV = Bone Volume. MIA = monoiodoacetate induced arthritis. VPG = Vesicular Phospholipid Gel.